Deep-Sea Research Vol 39 No 11/12, pp 1885–1917 1992
Printed in Great Britain

0198-0149/92 $5 00 + 0 00

An eastern Atlantic section from Iceland southward across the equator

MIZUKI TSUCHIYA,† LYNNE D TALLEY* and MICHAEL S. MCCARTNEY†

(*Received* 12 *April* 1991, *in revised form* 2 *December* 1991, *accepted* 16 *December* 1991)

Abstract—A long CTD/hydrographic section with closely-spaced stations was occupied in July–August 1988 from Iceland southward to 3°S along a nominal longitude of 20°W The section extends from the surface down to the bottom, and spans the entire mid-ocean circulation regime of the North Atlantic from the subpolar gyre through the subtropical gyre and the equatorial currents Vertical sections of potential temperature, salinity and potential density from CTD measurements and of oxygen, silica, phosphate and nitrate, based on discrete water-sample measurements are presented and discussed in the context of the large-scale circulation of the North Atlantic Ocean The close spacing of high-quality stations reveals some features not described previously The more important findings include (1) possible recirculation of the lightest Subpolar Mode Water into the tropics, (2) a thermostad at temperatures of 8–9°C, lying below that of the Equatorial 13°C Water, (3) the nutrient distribution in the low-salinity water above the Mediterranean Outflow Water that supports the previous conjecture of northern influence of the Antarctic Intermediate Water, (4) a great deal of lateral structure of the Mediterranean Outflow Water, with a number of lobes of high salinity, (5) an abrupt southern boundary of the Labrador Sea Water at the Azores–Biscay Rise and a vertically well-mixed region to its south, (6) a sharp demarcation in the central Iceland Basin between the newest Iceland–Scotland Overflow Water and older bottom water, which has a significant component of southern water, (7) evidence that the Northeast Atlantic Deep Water is a mixture of the Mediterranean Outflow Water and the Northwest Atlantic Bottom Water with very little input from the Iceland–Scotland Overflow Water, (8) an isolated core of the high-salinity, low-silica Upper North Atlantic Deep Water at the equator, (9) a core of the high-oxygen, low-nutrient Lower North Atlantic Deep Water pressed against the southern flank of the Mid-Atlantic Ridge just south of the equator, (10) a weak minimum of salinity, and well-defined maxima of nutrients associated with the oxygen minimum that separates the Middle and Lower North Atlantic Deep Waters south of the equator, (11) a large body of nearly homogeneous water beneath the Middle North Atlantic Deep Water between 20°N and the Azores–Biscay Rise, and (12) a deep westward boundary undercurrent on the southern slope of the Rockall Plateau

1 INTRODUCTION

LONG lines of deep, closely-spaced hydrographic stations with vertically continuous or high-resolution discrete measurements of water properties are of utmost importance to the study of the large-scale ocean circulation Such a line has been completed recently in the Atlantic Ocean along a quasi-meridional transect extending from Iceland (63°N) to South Georgia (54°S) One of the objectives for making this transect was to investigate in detail

Scripps Institution of Oceanography, University of California at San Diego, La Jolla, CA 92093-0230, U S A

†Woods Hole Oceanographic Institution, Woods Hole, MA 02543, U S A

the mid-ocean zonal circulation at all depths of the Atlantic Ocean, a pursuit severely hampered in the past by a lack of long meridional sections

Because of the extreme length of the transect, the field work was divided into two parts. The first was carried out in the North Atlantic in 1988 and the second in the South Atlantic in 1989. The purpose of this paper is to present vertical sections of properties observed during the first part and to describe and interpret various features of the property distributions in terms of the large-scale ocean circulation A companion paper based on data from the second part will be published at a later date.

The North Atlantic part of the transect (Fig 1) was occupied by R.V. *Oceanus* (OC202) in July–August 1988 with M. S. McCartney as Chief Scientist. The transect began at the shelf break immediately south of Iceland and extended along 20°W southward to 36°N northwest of Madeira. It then deflected to the west toward 20°N, 29°W, following the deepest portion of the eastern basin. After completing Sta 65 (33°19'N, 21°36'W), the observations were interrupted for 5 days by a port of call at Funchal, Madeira. From 20°N it ran due south along 29°W to 11°N, where it turned back to the southeast toward 1.5°N, 25°W. The equator was crossed along 25°W, and the southernmost station was occupied at 3°S. Except near its southern end, where it crossed the Mid-Atlantic Ridge, the section lies essentially in the eastern basin.

The station spacing was generally 56 km north of 30°N as well as between 1–3°S, and 83 km from 30 to 1°N It was reduced to 8–37 km over the slope south of Iceland and to 37 km over the steep topography just north of the Rockall Plateau, also within 1° of the equator On each station a rosette sampler equipped with a CTD was lowered to the bottom, and water samples were collected from 24 levels throughout the water column, except on a few shallow stations where the number of samples was reduced Frequent malfunctions of the closing mechanism of the rosette sampler during the first half of the cruise resulted in a loss of water samples at a considerable number of stations. Nevertheless, the vertical resolution of the discrete samples was generally satisfactory in water depths of <4000 m, but was coarser than desirable for the deeper stations which reached 5000–6000 m. Because of a problem with the autoanalyzer at the beginning of the cruise, no nutrient measurements (silica, phosphate, nitrate and nitrite) were made at Stas 1–6

Vertical sections of potential temperature, salinity and potential density (σ_θ and σ_2/σ_4), based on the CTD data, are presented in Figs 2–4, and those of dissolved oxygen, silica, phosphate and nitrate from bottle samples are presented in Figs 8–11 CTD oxygen was used sparingly to resolve a few features The CTD salinity was calibrated against the bottle salinity standardized with reference to P-108 standard seawater. The accuracies of the CTD pressure, temperature and salinity are better than 2–3 dbar, 0.002°C and 0.002 psu, respectively. Precision was 1 dbar, 0.001°C and 0.001 psu The accuracies of discrete measurements were 0.03 ml l^{-1} (0.5%) for oxygen, 2% for silica, and 1% for phosphate and nitrate; the fractional values are relative to the highest concentrations found in the regional water columns. The vertical exaggeration of the full-depth sections is 500, while that for the top 1.5 km, repeated in the upper panel, is increased to 1250. Potential vorticity (f/ρ) ($\partial\rho/\partial z$), shown in Figs 5–7, was calculated as described by TALLEY and MCCARTNEY (1982) using the Vaisala frequency, and hence, a reference density at each depth, the vertical derivative was calculated from a least-squares staight-line fit to the density profile with Gaussian weighting over a 60 dbar interval.

In the following sections, various features in the distributions of the properties illustrated in Figs 2–4 and 8–11 are described and interpreted in the context of the large-

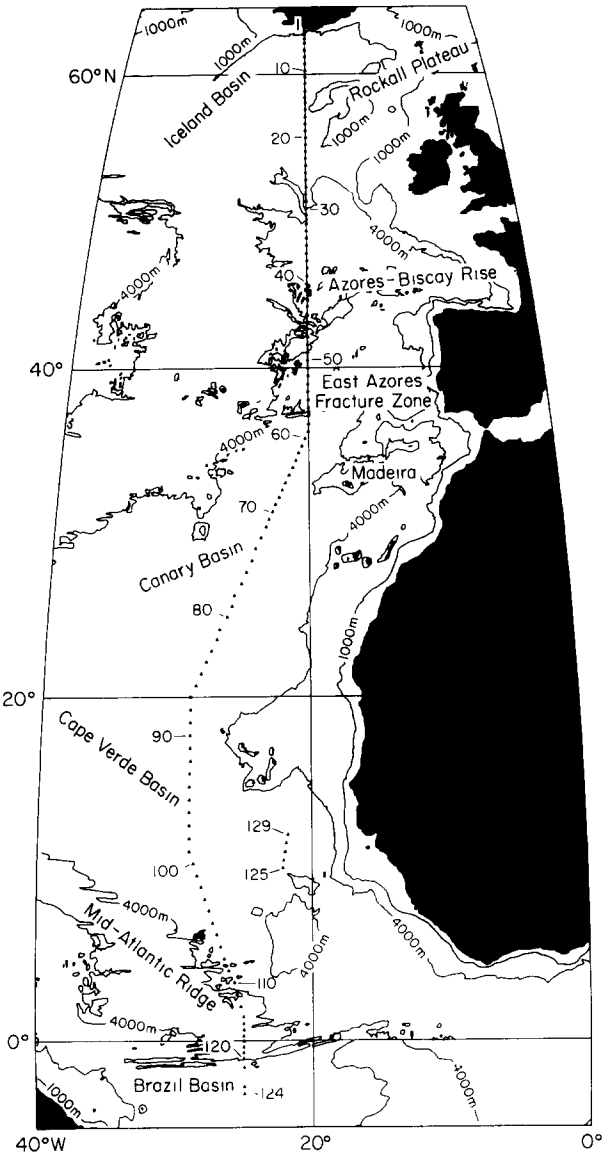

Fig 1 Station locations along the 20–25°W section occupied from north to south by R V *Oceanus* (OC202) between 23 July and 24 August 1988 The section was broken into two legs separated by 5 days between Stas 65 and 66

scale circulation of the North Atlantic Ocean The topics are arranged primarily by depth (surface to bottom) and secondarily by latitude (north to south). All density-anomaly values (σ_θ, σ_1,σ_2, etc.) quoted in this paper are calculated according to the International Equation of State (EOS80), with the units being kg m^{-3}. All salinity values are on the Practical Salinity Scale (PSS78). Table 1 lists the abbreviations of the water-mass names used in the text

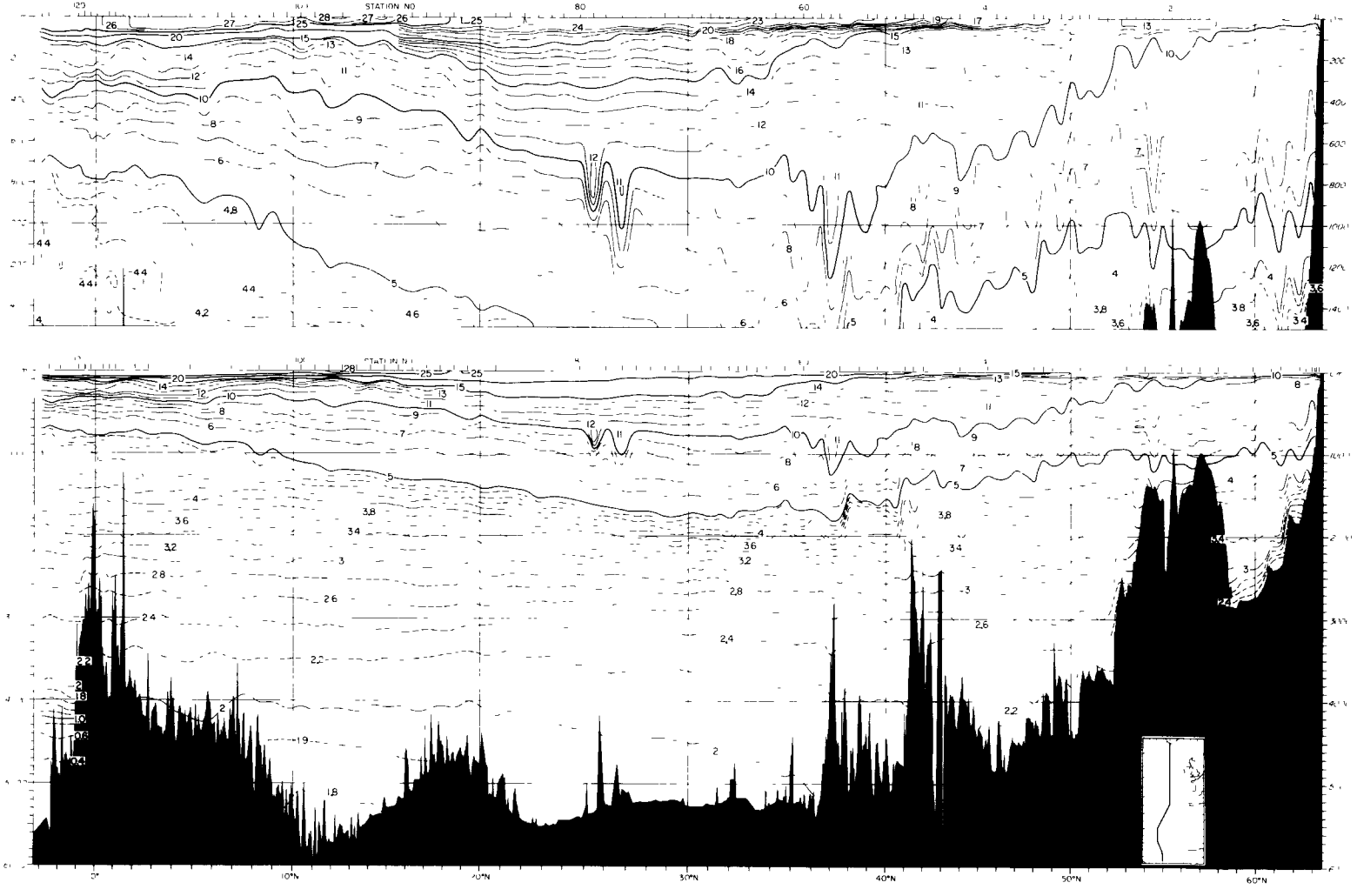

Fig 2 Vertical section of potential temperature (°C) from OC202, based on CTD data

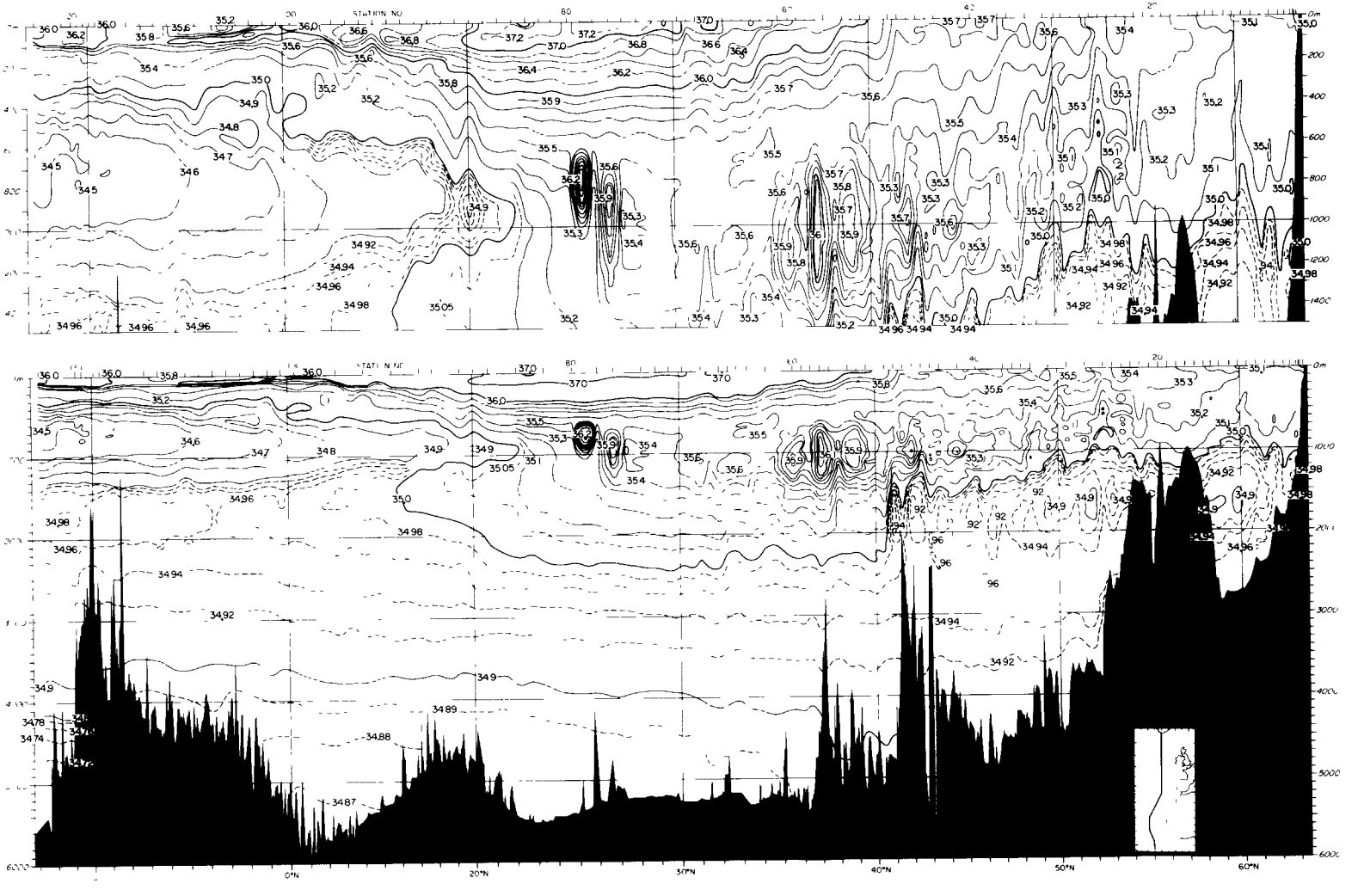

Fig 3 Vertical section of salinity from OC202, based on CTD data

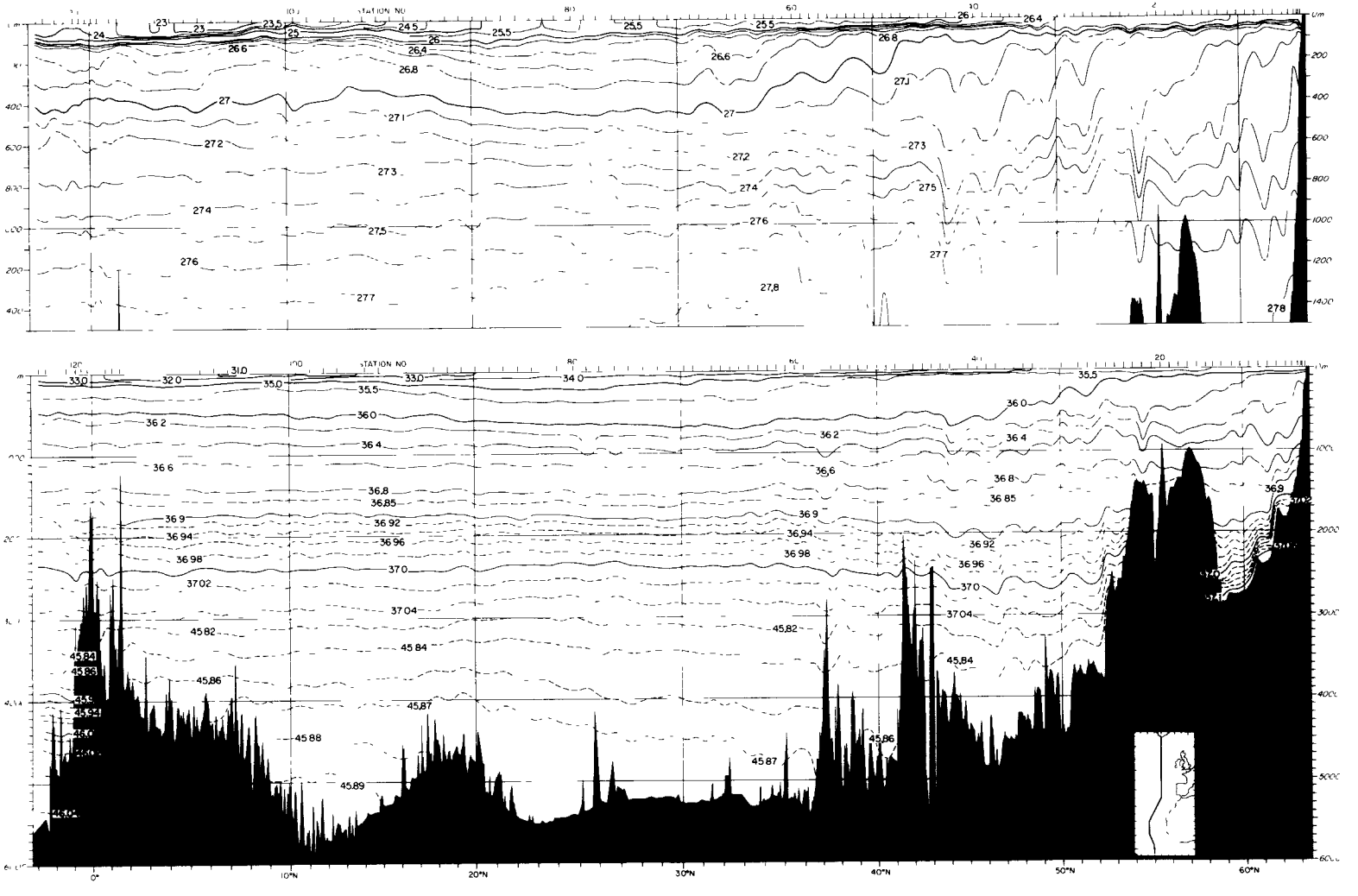

Fig 4 Vertical section of potential density (kg m^{-3}) from OC202, based on CTD data The upper section, covering the top 1500 m, shows σ_θ The full-depth section shows σ_2 for 0–3000 m and σ_4 for depths > 3000 m

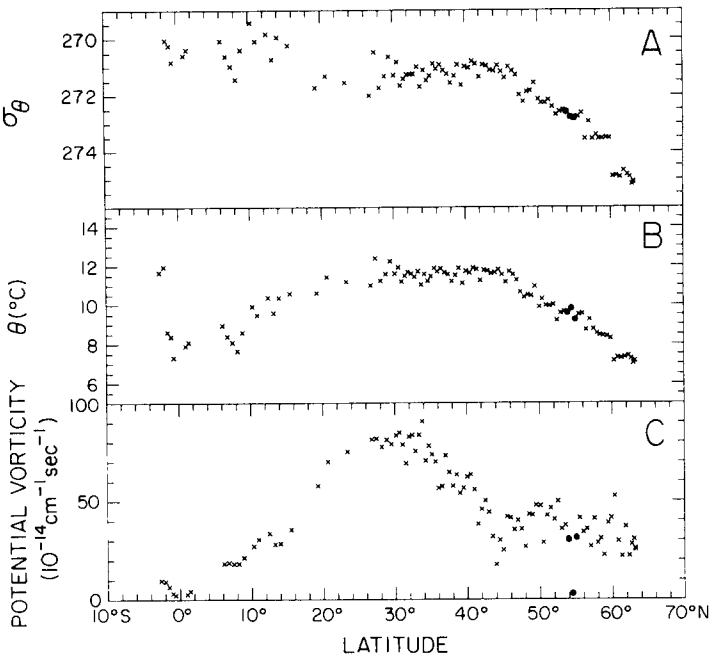

Fig 5 (A) σ_θ, (B) potential temperature (°C), and (C) potential vorticity (10^{-14} cm^{-1} s^{-1}) in the Subpolar Mode Water and equatorial and tropical pycnostads, as identified by a vertical minimum in potential vorticity calculated from CTD profiles along 20°W Stations used in Fig 7 are indicated with solid circles

2 SUBPOLAR MODE WATER

The Subpolar Mode Water (SPMW) is formed in the surface layer of the northern North Atlantic by deep winter convection. McCartney and Talley (1982) described its distribution and circulation, and changes in its temperature and density along the circulation path The SPMW first appears near 40–50°N, 38°W in its warmest form, and flows eastward with the North Atlantic Current. Part of it recirculates in an anticyclonic gyre east and south of the North Atlantic Current (McCartney, 1982), while the remaining water turns to the north to circulate counterclockwise in the northern North Atlantic The bulk of the latter portion ends up in the Labrador Sea, where it becomes the coldest, densest and thickest SPMW observed (This is the Labrador Sea Water discussed in Section 8.) The present section cuts through both of these circulation regimes.

On the vertical section of σ_θ, the pycnostad of the SPMW between 40 and 50°N is apparent at 11–12°C (σ_θ~27.1; salinity ~35.5; depth ~100–500 m) and in the Iceland Basin at 7.5°C ($\sigma_\theta \sim 27.5$, salinity ~35.15; depth ~100–700 m), with a monotonic transition between. Using its vertical potential-vorticity minimum as an identifier (Fig. 5), the SPMW can be defined in more detail. SPMW of 11–12°C (σ_θ~27.1) is found south of 47°N, extending all the way to about 27°N (Fig 5A), although vertical profiles of potential vorticity show only a weak pycnostad south of 40°N. From 47 to 60°N, the SPMW density increases to 27.35 σ_θ and potential vorticity remains uniformly low A sudden transition to 27 5 σ_θ occurs in the central Iceland Basin, with a concomitant drop in temperature from 8.5 to 7.5°C

On isopycnals that intersect the denser SPMW (e.g $\sigma_\theta = 27.3$ and 27.5 in Fig 6), a

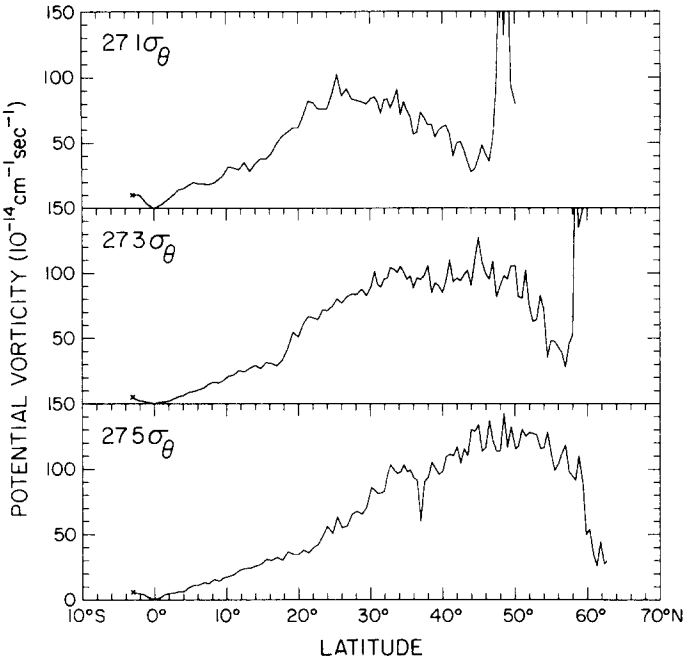

Fig 6 Potential vorticity (10^{-14} cm^{-1} s^{-1}) along isopycnals intersecting the Subpolar Mode Water calculated from CTD data along 20°W 27 1 σ_θ, 27 3 σ_θ, and 27 5 σ_θ

lateral minimum of potential vorticity occurs where SPMW is identified at that density. On the other hand, although the SPMW at 27.1 σ_θ occurs everywhere south of 47°N, a lateral minimum at this density occurs only at the northern end. This suggests that this SPMW forms in the north (McCARTNEY and TALLEY, 1982) and that it is this lowest-density SPMW which circulates into the subtropical gyre.

Although SPMW is the remnant of the winter mixed layer (McCARTNEY and TALLEY, 1982), summer stations do not usually show a well-mixed layer, in contrast to winter stations (ELLETT and MARTIN, 1973). At Sta. 22, however, we found a dramatically uniform mixed layer in the local SPMW density range (Fig. 7). SPMW potential vorticity at this station is also the lowest in the section (Fig. 5A). Station 22 is located at the southern edge of the Rockall Plateau, so the persistence of the mixed layer well past winter might be linked to the topography, for instance in a topographically-controlled eddy.

North of about 30°N, there is a general southward deepening of the upper-layer isopycnals, which indicates a broad eastward flow. This pattern is most notably interrupted by westward flows at 52–56°N and near 43°N. Superimposed on this background trend are vertical fluctuations of small horizontal scale, suggesting a high level of eddy activity in the region. Of course, it is not possible to infer the meridional motion of the SPMW from the present data

3 SUBTROPICAL AND TROPICAL HIGH-SALINITY WATERS

The highest salinities (>37.3) over the entire section are observed at the sea surface near 23°N, in a region of excessive evaporation Waters having salinities higher than 36 stretch

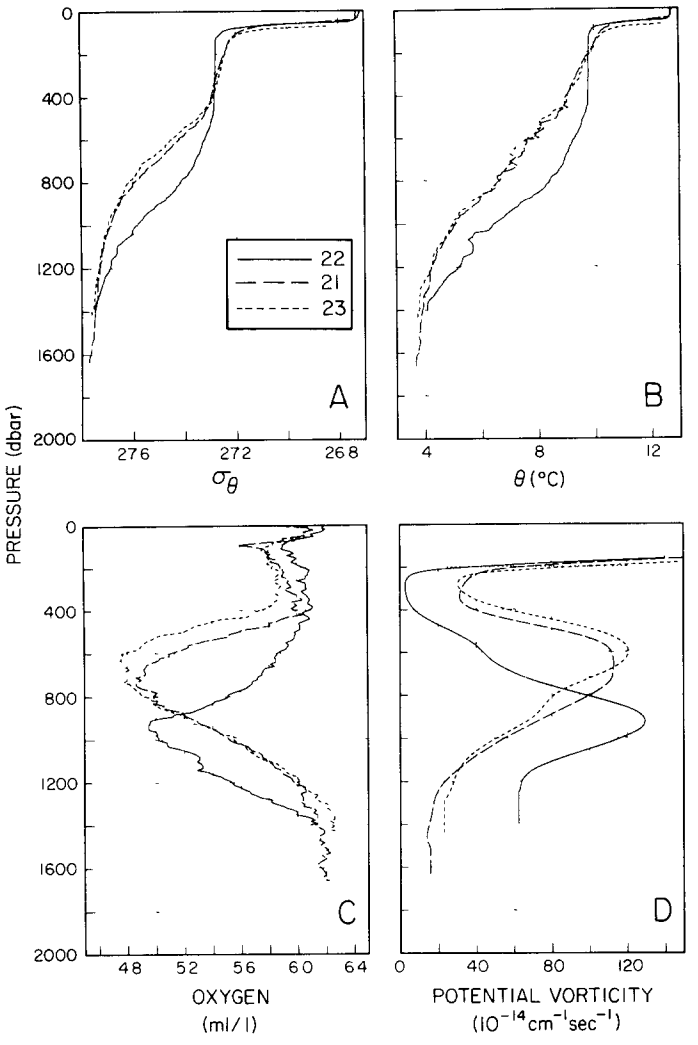

Fig 7 Vertical profiles of (A) σ_θ, (B) potential temperature (°C), (C) oxygen (ml l^{-1}), and (D) potential vorticity (10^{-14} cm^{-1} s^{-1}) from CTD data collected at Stas 21 (— — — 54°59′N), 22 (——— 54°29′N), and 23 (– – – – – 53°59′N) along 20°W

northward along the sea surface as far as 40°N, while exhibiting gradual decreases in temperature and salinity. Beneath this is a weak but clear indication of a 17–18°C thermostad ($\sigma_\theta \sim 26.5$) between 28 and 33°N. This thermostad may be identified as the Madeira Mode Water, formed by winter convection in the vicinity of Madeira, and separated from the 18°C Water of the western North Atlantic (Siedler *et al.*, 1987). The high-salinity water also extends southward as a subsurface tongue along $\sigma_\theta \sim 25.5$ to about 12°N, where the sea-surface temperature reaches its highest value of ~28.2°C. (Another tongue extending southward from 9°N is not a direct continuation of this tongue and will be described separately) There are at least three isolated high-salinity cores in the tongue, suggesting bands of alternating zonal flows, but the isopycnal slopes in the upper 500 m

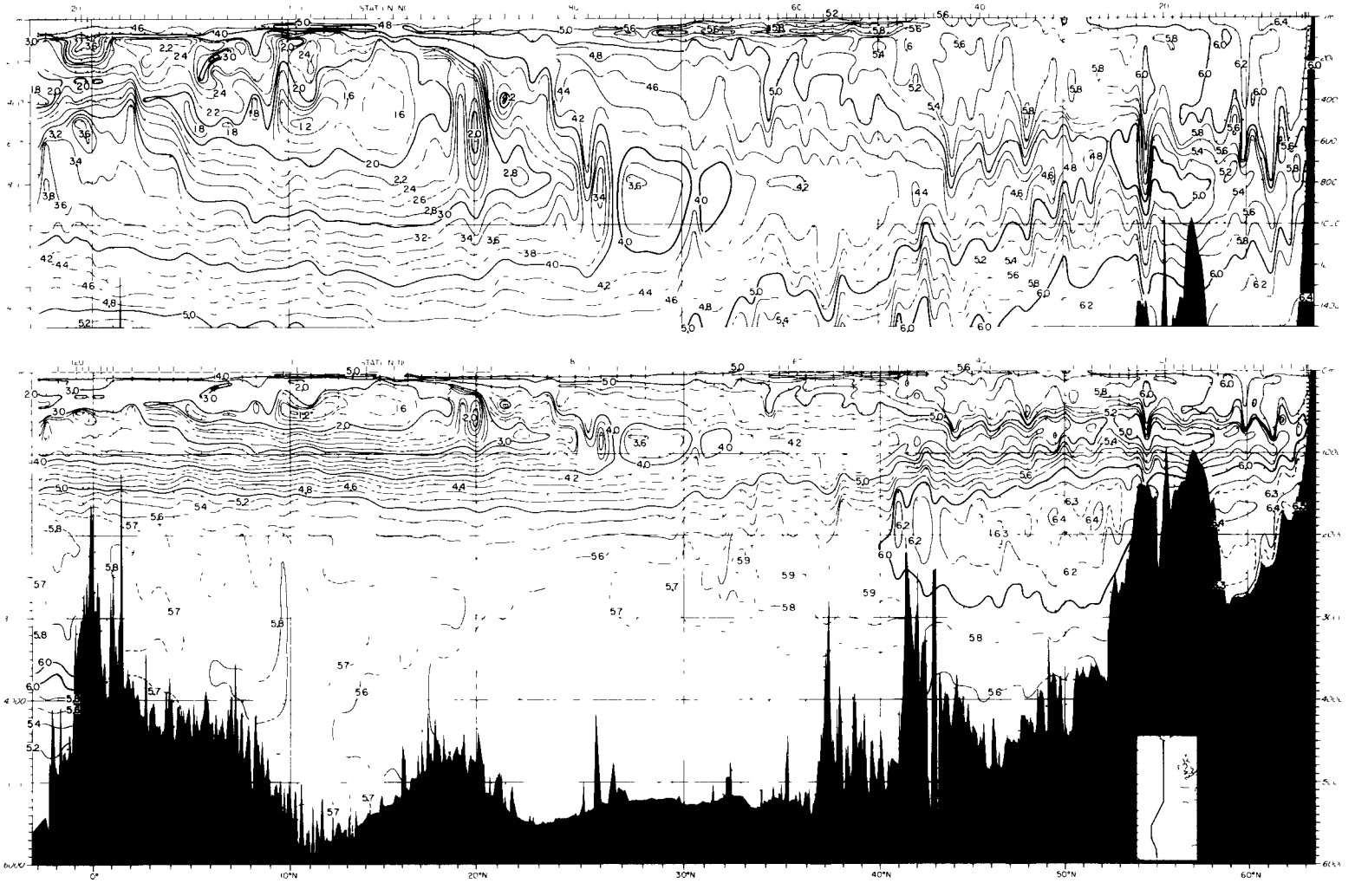

Fig 8 Vertical section of oxygen (ml l^{-1}) from OC202, based on discrete bottle data

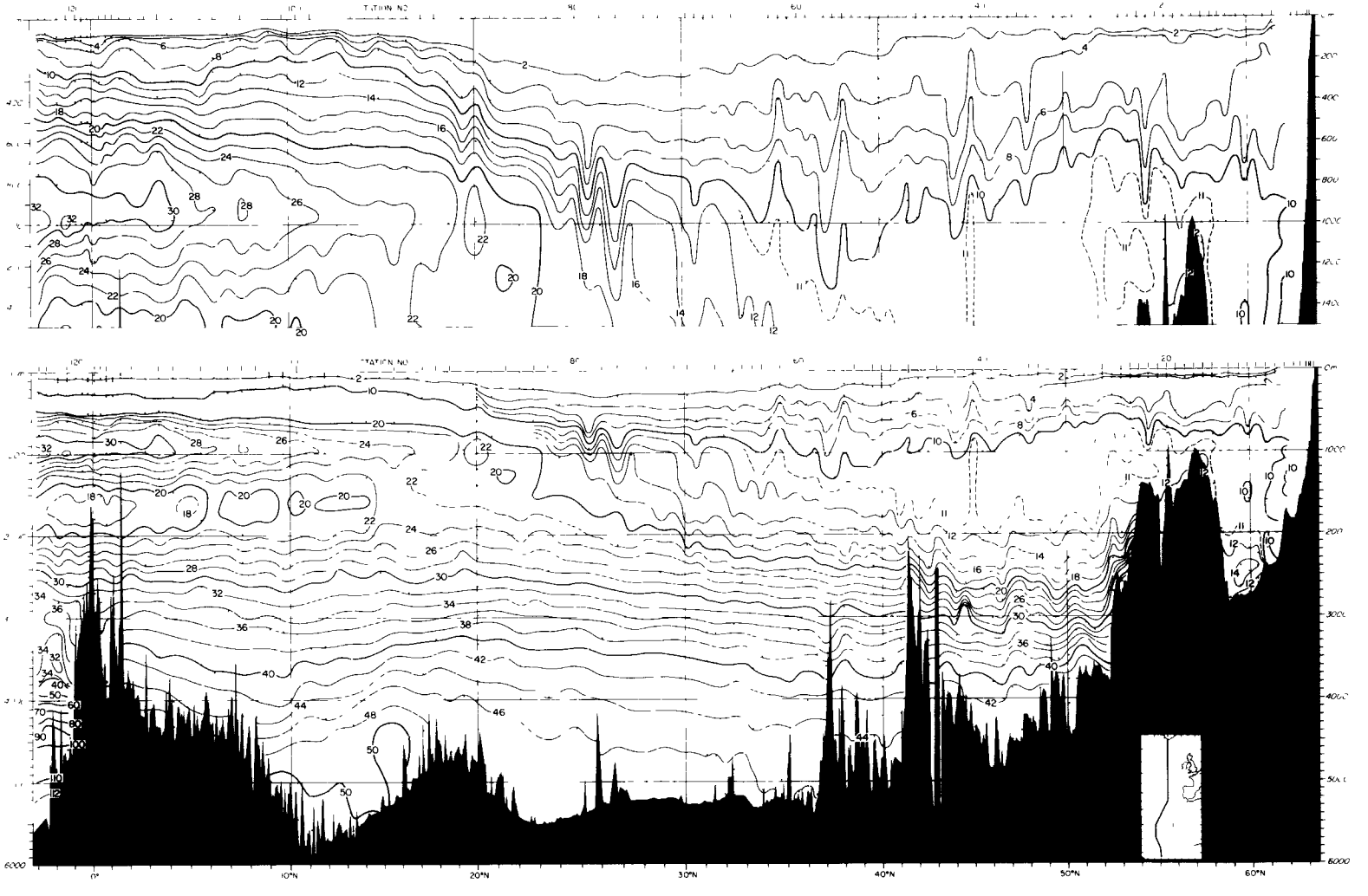

Fig 9 Vertical section of silica (μmol kg^{-1}) from OC202, based on discrete bottle data

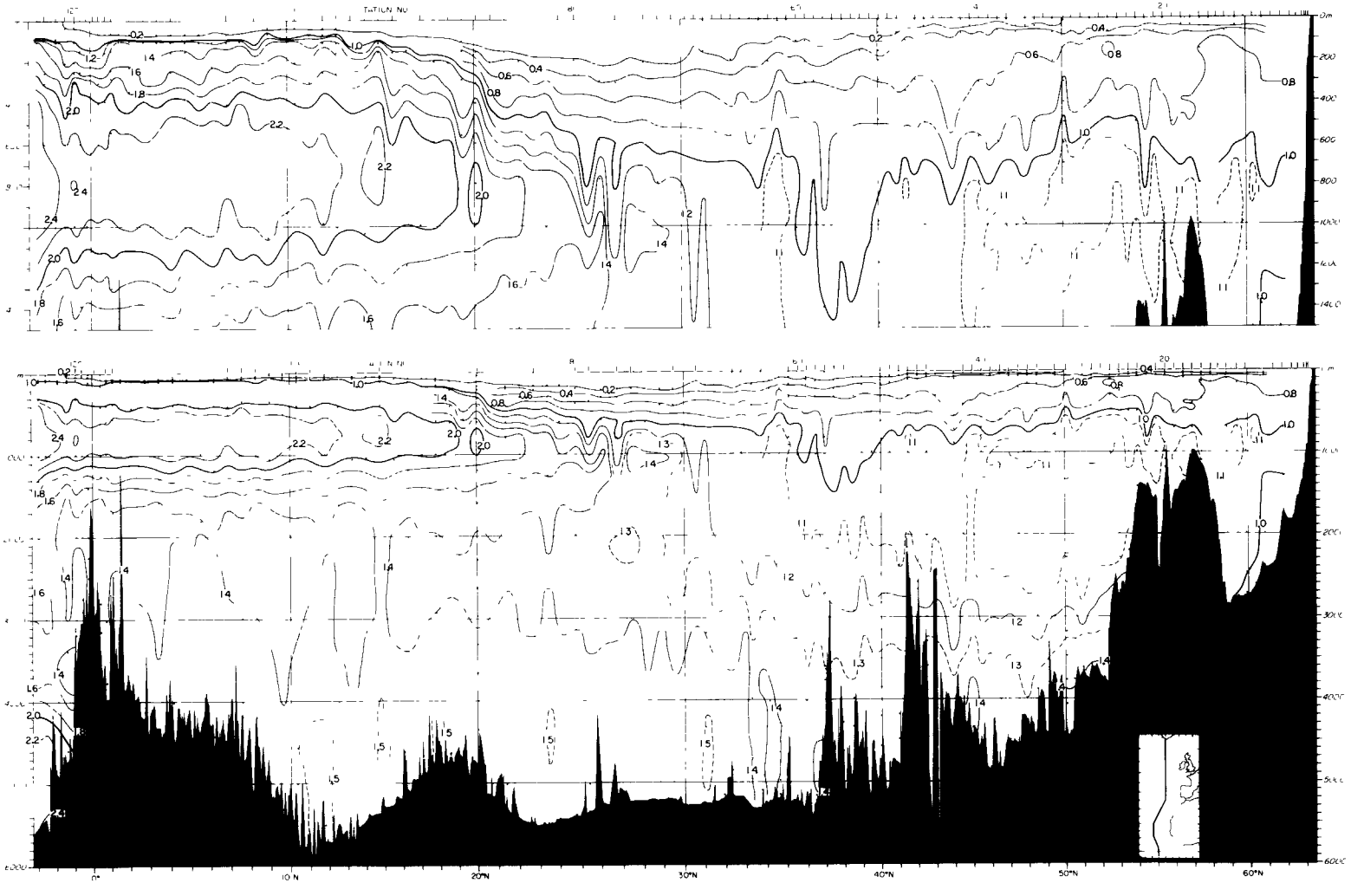

Fig 10 Vertical section of phosphate (μmol kg^{-1}) from OC202, based on discrete bottle data

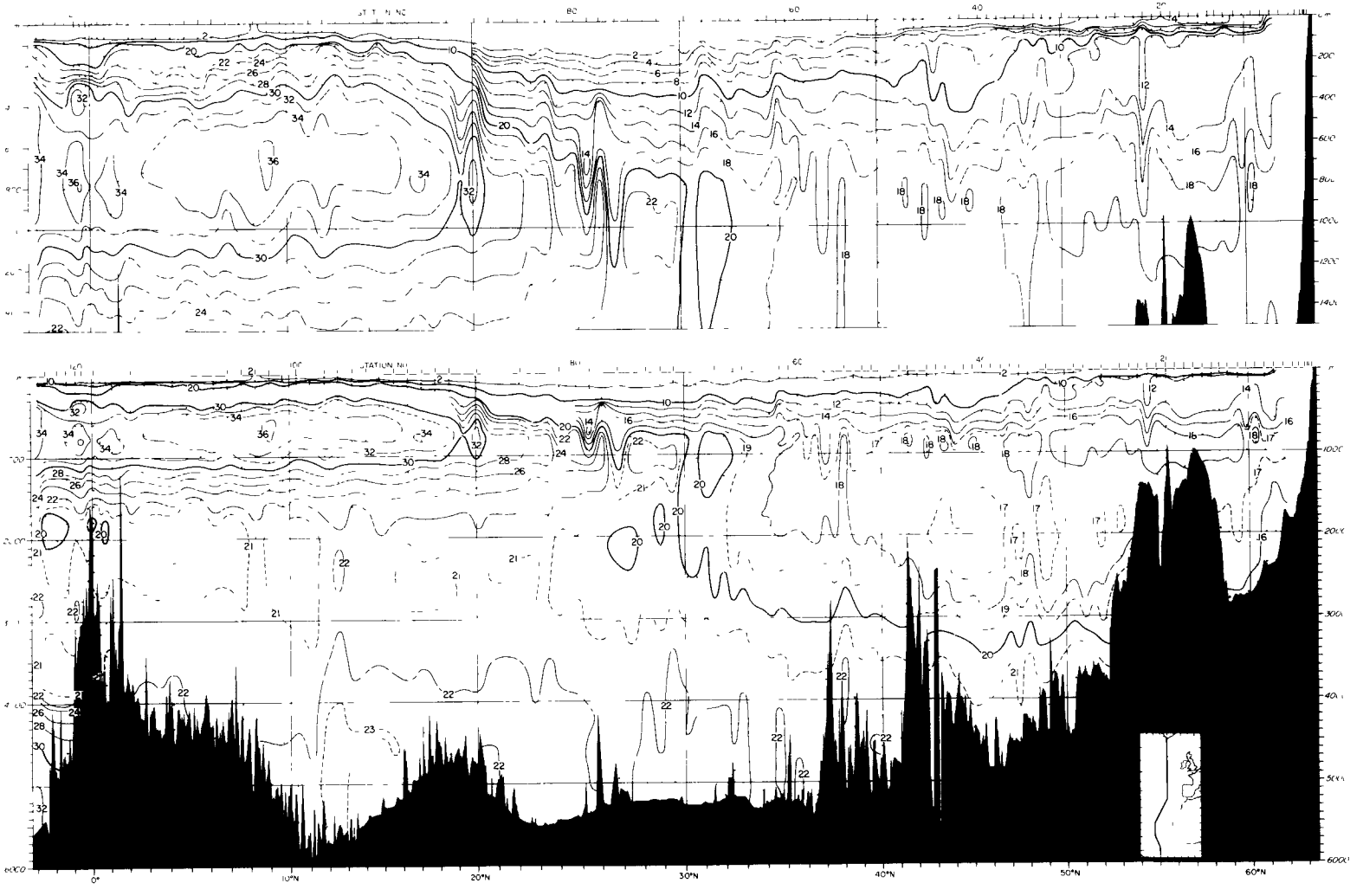

Fig 11 Vertical section of nitrate (μmol kg^{-1}) from OC202, based on discrete bottle data

Table 1 *Abbreviations of the water-mass used in the text*

Abbreviation	Full name
AABW	Antarctic Bottom Water
AAIW	Antarctic Intermediate Water
ISOW	Iceland–Scotland Overflow Water
LNADW	Lower North Atlantic Deep Water
LSW	Labrador Sea Water
MNADW	Middle North Atlantic Deep Water
MOW	Mediterranean Outflow Water
NADW	North Atlantic Deep Water
NEADW	Northeast Atlantic Deep Water
NWABW	Northwest Atlantic Bottom Water
SPMW	Subpolar Mode Water
UNADW	Upper North Atlantic Deep Water

indicate only a broad westerly flow of the North Equatorial Current, and hence that the saline cores are drifting with the large-scale flow

In the domain of this high-salinity water, the oxygen field exhibits a clearly defined vertical maximum at 30–100 m, with the water above it being supersaturated (generally ~103%, but up to 110% in some places) This shallow subsurface maximum of oxygen has been observed in summer in both Atlantic and Pacific Oceans (REID, 1962) and can be explained by photosynthetic production of oxygen that remains trapped beneath the strong density gradient created by summer warming of near-surface water (SHULENBERGER and REID, 1981; JENKINS and GOLDMAN, 1985, CRAIG and HAYWARD, 1987).

Another high-salinity tongue begins at the sea surface near the northern boundary of the North Equatorial Countercurrent, which is indicated by the equatorial deepening of the pycnocline from 9 to 3°N. The tongue extends equatorward to 2°N along $\sigma_\theta \sim 24.5$ in the sharply developed pycnocline, and contains salinities >36.1, with the highest value (~36.3) being at 40 m near 8°N. The high-salinity core is overlain by low-salinity equatorial surface water (<35.8) associated with high precipitation in these latitudes. No salinity as high as in the core is found at the sea surface just to the north where the tongue originates. Similar high-salinity cores in the North Equatorial Countercurrent have been found in earlier data from the equatorial Atlantic (KOLESNIKOV, 1973; BUBNOV *et al.*, 1979; DUING *et al.*, 1980; KHANAICHENKO, 1980; HENIN *et al.*, 1986), and are consistent with the eastward flow of high-salinity water, which appears to contain a significant amount of South Atlantic water that crosses the equator north of Brazil (MONTGOMERY, 1938, MERLE, 1978)

On the southern edge of the high-salinity core, salinity along isopycnals near this σ_θ (24 0–25.0) reaches a lateral minimum and increases again farther south An isolated high-salinity core (>36.2) is found to be centered at 70 m ($\sigma_\theta \sim 24.5$), slightly south of the equator. This core is obviously associated with the Equatorial Undercurrent, which transports high-salinity, high-oxygen water of South Atlantic origin eastward (METCALF and STALCUP, 1967). The salinity maximum of the Equatorial Undercurrent is, on average, 30 km south of the velocity maximum (FAHRBACH *et al.*, 1986), and the current axis can migrate by $\frac{1}{2}°$ either side of the equator (DUING *et al* , 1975), thus accounting for our salinity core as being ~75 km south of the equator. The Equatorial Undercurrent is also seen clearly as troughs of the subthermocline isopycnals and isopleths of oxygen and nutrients extending down to 300 m

4 EQUATORIAL THERMOSTADS AND SUBTHERMOCLINE CURRENTS

The thermostad of the Equatorial 13°C Water ($\sigma_\theta \sim 26.6$) is well developed from 5°N to the southern end of the section (3°S). However, the thermostad's mean temperature varies with latitude. It is 13°C at 3–5°N, 12.5°C at 1–3°N, and 13–13.5°C south of 1°N. As was noted in previous studies (HISARD *et al.*, 1976; KELLEY, 1978, TSUCHIYA, 1986), the thickness of the thermostad (as measured by the vertical separation of the 12 and 14°C isotherms, for example) exhibits maxima north and south of the equator with a minimum at the equator

On the northern side of the thermostad is the subsurface (or subthermocline) North Equatorial Countercurrent (COCHRANE *et al.*, 1979), indicated by the steep equatorward dip of the subthermocline isotherms for 9–14°C. The eastward flow of the subsurface Countercurrent appears to extend to that of the shallower (surface) North Equatorial Countercurrent without showing a subsurface speed maximum. However, it is distinctly separated from the Equatorial Undercurrent by a westward flow described just below. The subsurface Countercurrent is associated with an isolated subthermocline high-oxygen core (>3 ml l^{-1}) at $\sigma_\theta \sim 26$ 7, which is consistent with the transport of high-oxygen water from the west (COCHRANE, 1975; MERLE, 1978; TSUCHIYA, 1986) The nutrient fields show only weak minima in the core.

The subsurface South Equatorial Countercurrent is just barely visible in the slope of the same subthermocline isotherms at the southern end of the section.

Between 1.5 and 5°N the slope of the subthermocline isotherms indicates that flow is westward here. This sense of flow immediately north of the Equatorial Undercurrent is consistent with an isolated core of low oxygen (<2.2 ml l^{-1}) at 100–200 m, just beneath the primary thermocline, because the only source of low oxygen near this density level is to the east (MONTGOMERY, 1938; MERLE, 1978, TSUCHIYA, 1986) This is also consistent with the lateral minimum of salinity in the pycnocline (Section 3), which suggests a westward flow from the low-salinity region in the eastern equatorial Atlantic by way of the northern portion of the South Equatorial Current.

In the upper layer of the equatorial region, there are two other thermostads (pycnostads) not noted previously (Figs 2, 4 and 5) Both thermostads are not defined as well as that of the 13°C Water, but are clearly recognized in the present data. One occurs at 8–9°C ($\sigma_\theta \sim 27.05$; depth ~400 m) within about 2° of the equator. It lies just beneath the secondary thermocline which marks the bottom of the 13°C Water thermostad. Vertical sections of temperature along 13.5 and 18.5°W, presented by METCALF *et al.* (1962), and some of the meridional sections occupied between 35°W and 6°E during the FOCAL (Français Océan et Climat Atlantique équatorial) program in 1982–1984 (HENIN *et al.*, 1986) also show this thermostad at and near the equator. Its cause and significance are not known

The other new thermostad is found at about the same depth between 6 and 15°N, but at a slightly lower density ($\sigma_\theta \sim 27.0$) The pycnostad temperature is ~9°C in the south and ~10°C in the north. A similar pycnostad was observed at $\sigma_\theta \sim 27.1$–27 2 east of 25°W, in a section along 24°N, by ROEMMICH and WUNSCH (1985). Because both of these pycnostads occur in the density range of the warmest form of the SPMW (MCCARTNEY, 1982; MCCARTNEY and TALLEY, 1982), the pycnostad observed at 6–15°N in the present section might represent the recirculation of the SPMW in the subtropical gyre. Further investigation is required to confirm this conjecture

5 LOW-SALINITY WATER OVERLYING THE MEDITERRANEAN OUTFLOW WATER

There is a vertical minimum of salinity at about 500–800 m, embedded between the high-salinity subtropical water above (Section 3) and the Mediterranean Outflow Water (MOW) below (Section 7) It can be recognized most clearly between 32 and 42°N (Sta. 47–68), where the MOW is best developed, but extends farther north and south in a less distinct form. The minimum is also well defined above the isolated Mediterranean salt lenses or Meddies (McDOWELL and ROSSBY, 1978) observed at Stas 77 and 79, near 26–27°N (Section 7).

In the region where the salinity minimum is well developed, the minimum occurs at $\theta \sim 10$–11°C, $\sigma_\theta \sim 27.2$–27.4 and $\sigma_1 \sim 31\ 6$–31 8 (Fig. 12). The minimum salinities are 35.5–35.6, and the laterally lowest salinities are observed at 32–34°N and near 41°N, although the distribution is somewhat patchy.

North of 42°N, the minimum is less clearly defined and not well depicted by the isohalines in the section; it is only barely recognizable at some stations. Nevertheless, it still exists at a somewhat lower temperature ($\theta \sim 8$–10°C; $\sigma_\theta \sim 27.4$–27 5) to as far north as 54°N (Sta. 23). This northward extension of the salinity minimum is of course associated with the overlying high-salinity water of subtropical origin and with the underlying high-salinity MOW, which is flowing northward along the European coast (Section 7).

South of 30°N, the minimum shifts to lower temperatures. At 22°N (Sta. 84) the minimum is intensified (<35.0) and located at $\theta \sim 6$°C ($\sigma_\theta \sim 27.5$). Southward of this station, the minimum is identifed as the Antarctic Intermediate Water (AAIW) extending northward from the South Atlantic (Section 6).

North of 30°N, the low-salinity water has been thought to originate in the northern North Atlantic. WUST (1935; see his Beilage XXIII) called this salinity minimum the North Atlantic Intermediate Water and, on the basis of very limited data, he inferred its primary formation region to be over the Davis Strait sill. Recently, ARHAN (1990) discussed its source and subduction into the subtropical region in the light of new hydrographic data and the ventilated thermocline theory of LUYTEN *et al.* (1983), and suggested that it originates in the Labrador Current. The patchy salinity distribution in the minimum on the present section suggests that it may be coming from the west along zonal flows or that there are numerous eddies in this region. A map of salinity on an isopycnal ($\sigma_1 = 32.0/\sigma_\theta = 27.48$), coinciding roughly with the salinity minimum (TSUCHIYA, 1989) shows low-salinity water extending from the Labrador and Irminger Seas southward along the western boundary and also eastward along about 50°N However, from the distribution of silica on the same isopycnal, he showed that the AAIW flows northward along the western boundary of the North Atlantic and then leaves the boundary along the Gulf Stream–North Atlantic Current It reaches 50–60°N south of Iceland. Thus it is possible that the low-salinity water above the MOW contains a significant amount of the AAIW transported by the Gulf Stream–North Atlantic Current along the west and north edges of the MOW. The isolated core of low salinity (<35.5) centered at 34°N (Fig 3) may represent another branch of eastward flow of the low-salinity AAIW that has separated from the western boundary at a lower latitude

6 ANTARCTIC INTERMEDIATE WATER

The low-salinity tongue of the AAIW extends as a strong feature at about 600–800 m from the south end of the section to about 22°N At 3°S the salinity minimum is located at

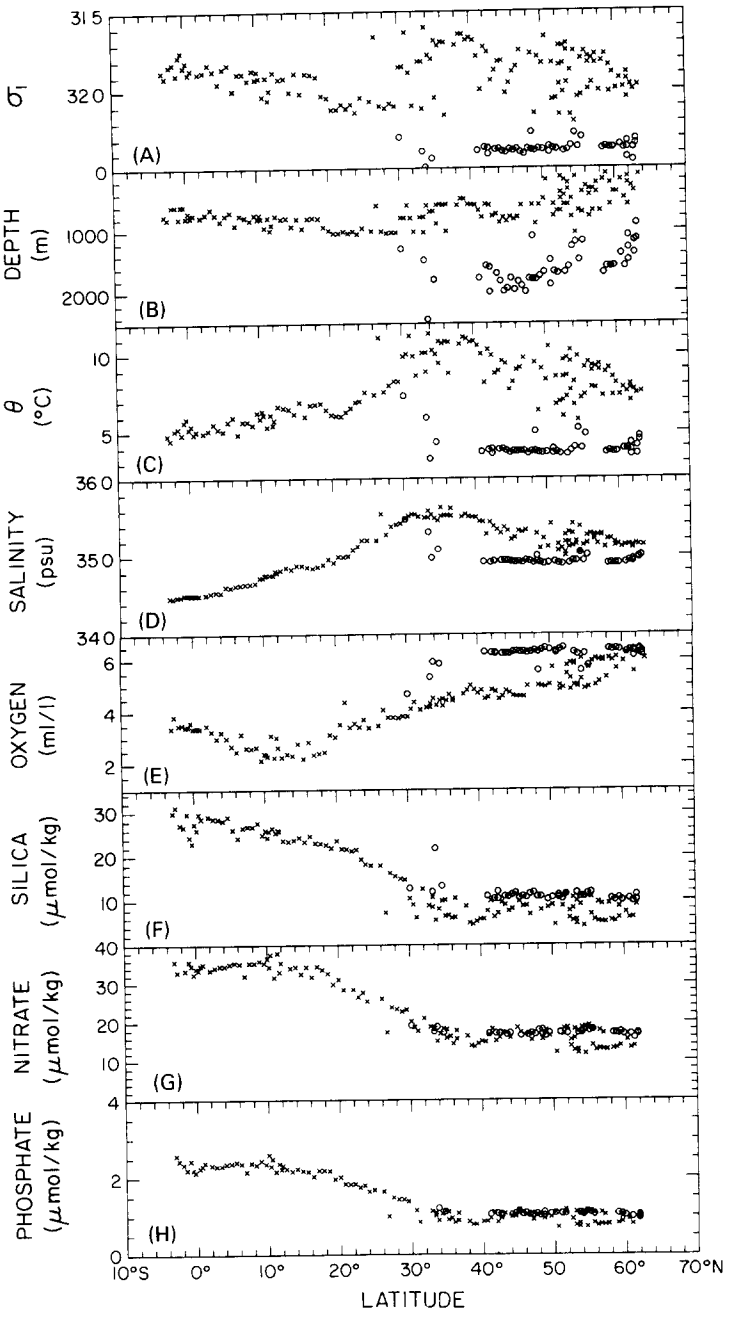

Fig 12 (A) σ_1, (B) depth (m), (C) potential temperature (°C), (D) salinity, (E) oxygen (ml l^{-1}), (F) silica (μmol kg^{-1}), (G) nitrate (μmol kg^{-1}), and (H) phosphate (μmol kg^{-1}) at all salinity minima found between 31 6 and 32 25 σ_1 (×) and between 32 25 and 32 5 σ_1 (○), based on discrete bottle data South of 30°N this minimum is identified as the AAIW (Section 6) Between 30 and –40°N, the shallower salinity minimum overlies the MOW (Section 5) North of 40°N, the shallower minima are in a strong interleaving regime above the LSW The deeper salinity minimum (○) is predominantly LSW (Section 8)

$\theta \sim 5°C$ ($\sigma_\theta \sim 27.3$), with salinity < 34.5 (Fig. 12). Potential temperature, salinity and σ_θ in the AAIW increase to the north, the latter due to the greater influence of increasing salinity relative to potential temperature. Oxygen decreases northward to a minimum at 12–19°N, while phosphate and nitrate are nearly uniform south of 20°N The oxygen distribution is heavily influenced by water from the well-known low-oxygen domain in the eastern equatorial North Atlantic (e g MERLE, 1978) and does not show any vertical extremum in the AAIW over most of our section. There is, however, an isolated core of high oxygen (>3.4 ml l^{-1}) centered at about 550 m (σ_θ~27 1), slightly above the salinity minimum just south of the equator. This high-oxygen core also is recognized as a tongue extending eastward along the equator on maps of oxygen in the AAIW (WUST, 1935; REID, 1989)

North of 22°N, a weak minimum continues to Sta. 80 (25°N), where its σ_θ is about 27 55. Its continuity is interrupted by the Meddies at Stas 79 and 77, but it is still visible at Stas 75 and 76 (Fig 3). Oxygen, as well as temperature and salinity, increases to the north in this weak minimum, suggesting that it is not a simple northward extension of the stronger AAIW encountered farther south on this section. As described in Section 5, a strong salinity minimum, which is distinct from this weak AAIW and overlies the MOW, is first encountered above the Meddies at Stas 77 and 79 (26°N) and is a coherent feature from station to station between 32 and 45°N (Stas 67–41).

The AAIW in the equatorial Atlantic is characterized by relatively high silica concentrations (METCALF, 1969; MANN *et al* , 1973; BAINBRIDGE, 1980; TSUCHIYA, 1989). A well-defined tongue of high silica extends northward, approx. 150 m below the AAIW salinity minimum It lies at $\sigma_\theta \sim 27$ 4 at 3°S, and at $\sigma_\theta \sim 27.5$ near 23°N, where the tongue terminates The silica maximum associated with the AAIW is not present between 24 and 40°N, but north of 40°N a weakly defined maximum appears at $\sigma_\theta \sim 27.6$–27.7 ($\sigma_1 \sim 32.2$), though not revealed everywhere by the isopleths on the section. This is in contrast to that seen in the GEOSECS (Geochemical Ocean Sections Study) western Atlantic section, which shows a continuous high-silica tongue extending north to 50°N (BAINBRIDGE, 1980). No coherent salinity minimum is associated with this maximum Properties at the northern silica maximum show decreasing temperature and salinity to the north, increasing oxygen, and nearly uniform phosphate, silica and nitrate. This northern maximum can be explained by the transport of the high-silica AAIW from the west along the Gulf Stream–North Atlantic Current (Section 5).

There are similar tongues of high phosphate and nitrate extending northward to about 30°N Near the equator these tongues are just beneath the salinity minimum, but north of about 9°N they are generally shallower. The silica, phosphate and nitrate maxima are patchy It is tempting to interpret these patches of high nutrients as indicating eastward zonal flows, but the patches of the three nutrients do not coincide with each other everywhere.

Similar to silica, weak maxima of phosphate and nitrate appear again north of 40°N but are slightly shallower than the silica maximum. The phosphate and nitrate maxima north of 40°N are consistent with the contribution of the AAIW suggested by the silica field.

7 MEDITERRANEAN OUTFLOW WATER

The highly saline MOW is clearly seen between 30 and 42°N, with its strongest development (maximum salinity >36.1) at 37°N (Sta. 57). Its core is located at 9–10°C

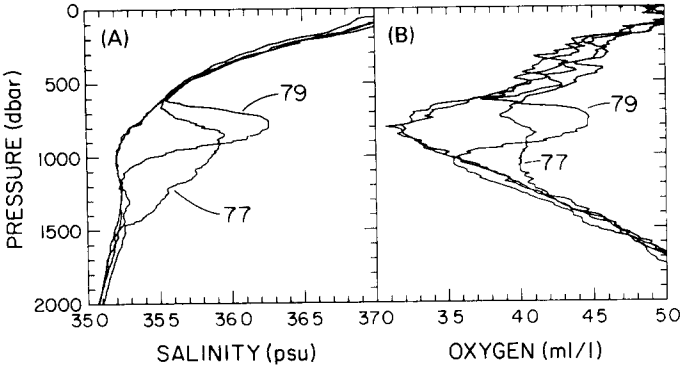

Fig 13 (A) Salinity and (B) oxygen (ml l^{-1}) in the Meddies at Stas 77 and 79 Stas 78 and 80 are also shown for comparison

($\sigma_\theta \sim 27\ 7$; $\sigma_1 \sim 32.1$, depth ~1000 m) Between 35 and 40°N a well-developed thermostad (not a pycnostad) nearly 500 m thick occurs at 10–11°C in the upper portion of the MOW. At some stations, there is a temperature maximum in the thermostad.

South of 30°N, a slight maximum in salinity is still observed at progressively lower temperatures, though not apparent in the section At 25°N it is found at $\theta \sim 6$°C ($\sigma_\theta \sim 27.7$; $\sigma_1 \sim 32.3$; depth ~1300 m). Two isolated lenses of the MOW (Meddies) are observed at Stas 77 and 79, at 25–27°N (Fig. 13). Salinity (>36.2) at the Sta. 79 Meddy is the highest observed in the MOW. The MOW at both Meddy stations has anomalously high temperature (>11°C) and low density (σ_1~31.8–31.9) compared with MOW at all other stations. These Meddies are part of a general pattern of Meddy occurrences in an elliptical region extending about 3000 km southwest from Portugal (Richardson *et al.*, 1991), intersected by our section between 19–41°N. The oxygen content of the Meddies that we observed is anomalously high on isopycnals (1.0–1.4 ml l^{-1} higher than neighboring stations), but is about the same as non-Meddy MOW Information on whether oxygen is generally higher in Meddies is lacking; the Armi and Stommel (1983) observations from 1978–1980 show higher oxygen in the Meddies, but the Armi and Zenk (1984) observations from 1981 do not show any enhancement.

Irregular staircases in temperature, salinity and density are evident below the salinity maximum at many stations between 29°30′–39°N and also beneath the Meddies (Fig. 14). The most regular staircases, with steps 20–50 m thick, occur south of the highest-salinity MOW, over a depth range of about 500 m The density range for the staircases is $\sigma_1 \sim 32.35$–32.45 and $\sigma_2 \sim 36.75$–36.95. Density ratios for this range of σ_2 (Fig. 15) are <2, indicating the potential for salt-fingering (Schmitt, 1981). The large region in which staircases are found suggests large-scale mixing between MOW and the overlying LSW, discussed in the next section

Southward from 22°N the salinity maximum is again well defined at $\theta \sim 4$–5°C ($\sigma_\theta \sim 27\ 7$–$27\ 8$) because of the presence of the low-salinity tongue of the AAIW in the layer just above. This broad salinity maximum centered at 1500–1800 m is the Upper North Atlantic Deep Water defined by Wust (1935), and will be described in Section 11 On the other hand, the northward extension of the MOW is recognized as far north as nearly 50°N, at about the same density ($\sigma_\theta \sim 27.6$) but at a lower temperature ($\theta \sim 7$°C). Reid (1979) has shown that the MOW extends northward along the coast of Europe as well as

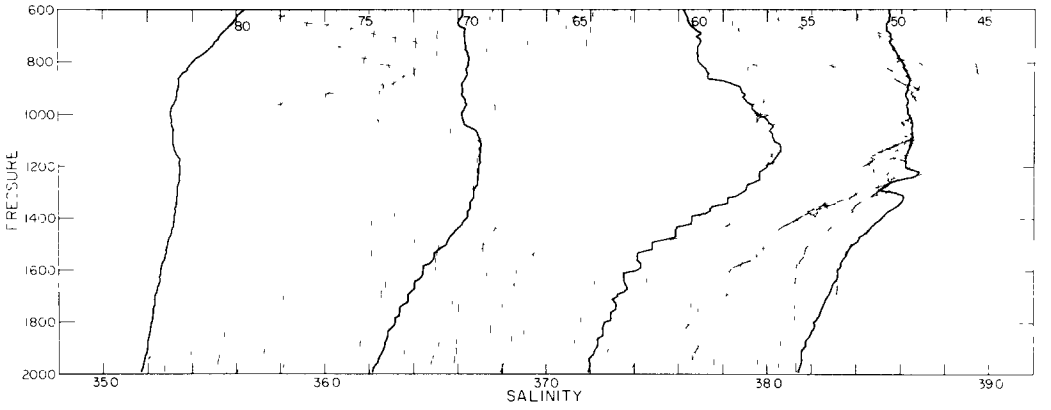

Fig 14 Salinity as a function of pressure (dbar) for Stas 45–81 Salinity scale is correct for Sta 81, each subsequent station in decreasing order is offset by 0 1 psu Stas 80, 70, 60 and 50 are indicated by heavy curves

westward. However, the salinity distribution here is irregular and shows a great deal of small-scale structure. A distinct maximum does not occur at every station.

A vertical minimum of oxygen at $\sigma_\theta \sim 27.5$ ($\sigma_1 \sim 32.0$) is apparent somewhat above the MOW. The minimum extends all the way to the northern end of the section. Unlike salinity, however, oxygen does not provide a distinctive signature of the MOW. On isopycnals intersecting the MOW, oxygen shows a monotonic northward increase in concentration, and an area of lower oxygen extends northward along the coasts of Africa and Europe (REID, 1979). This lower-oxygen water has its source in the oxygen-depleted domain of the eastern equatorial North Atlantic, which is recognized in our section as the core of low-oxygen water (<1.8 ml l^{-1}) just below the pycnocline between 9–18°N. The

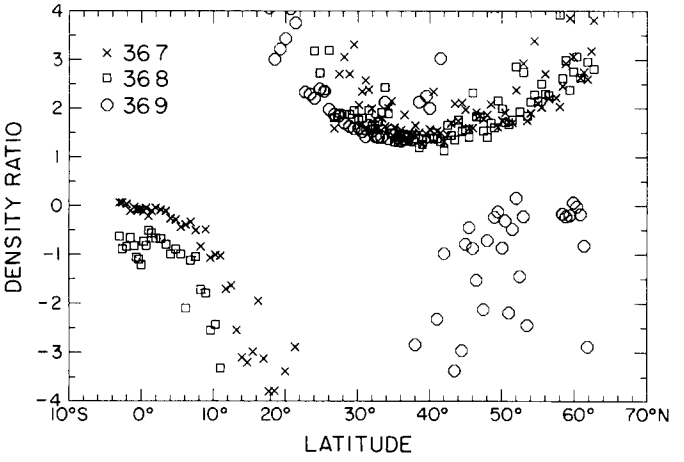

Fig 15 Density ratio $(\alpha\partial T/\partial p)/(\beta\partial S/\partial p)$, where $\alpha = -\rho^{-1}\ \partial\rho/\partial T$ and $\beta = \rho^{-1}\ \partial\rho/\partial S$, on σ_2 isopycnals which lie below the MOW and above the LSW (36 7, 36 8 σ_2) and just below the LSW (36 9 σ_2) Positive values <2 suggest that salt-fingering is active (SCHMITT, 1981)

vertical minimum of oxygen apparently associated with the MOW is influenced by the deep portion of this low-oxygen water.

8 LABRADOR SEA WATER

The Labrador Sea Water (LSW) is characterized by a salinity minimum and a pycnostad (thermostad) at about 1500 m, and is found from Sta. 7, near the northern end of the section, to Sta. 49 (41°N) just south of the Azores–Biscay Rise. Its minimum salinity is <34.94 almost everywhere, reaches to < 34 90 at some locations, and averages 34.91 The average potential temperature at the minimum is 3.55°C and is close to the value (3.5°C) quoted by WORTHINGTON and METCALF (1961) for the LSW north of 40°N The average σ_2 at the salinity minimum along the present section is 36.87 ($\sigma_\theta \sim 27.76$).

Although the θ–S and σ_2–S relations are tight between Stas 7 and 49, salinity of the LSW in this region is marginally lowest just north and south of the Rockall Plateau, both coinciding with highest oxygen as well These match the distribution of the LSW on isothermal or neutral surfaces (WORTHINGTON and WRIGHT 1970, Plates 37 and 39; IVERS, 1975, Fig. 17) and the TALLEY and MCCARTNEY (1982) description of the main eastward flow of the LSW across 20°W near 50°N with an additional branch as part of a cyclonic circulation in the Iceland Basin. The isopycnal slopes (Fig. 4) also suggest a cyclonic circulation of LSW in the Iceland Basin if a level of no motion is taken below the LSW.

The mid-depth oxygen maximum found all along the section was denoted Middle North Atlantic Deep Water (MNADW) by WUST (1935) North of 41°N, the oxygen maximum is clearly associated with the LSW's salinity minimum. The average concentration of oxygen at the maximum is 6.34 ml l^{-1} for Stas 1–49, with the highest value above 6.4 ml l^{-1}. The average density of the oxygen maximum is 36.89 σ_2, which is slightly greater than at the salinity minimum. The salinity minimum is also associated with weak minima of silica, phosphate and nitrate, but these nutrient minima are less clearly defined than the oxygen maximum and are not found south of the salinity minimum. The silica minimum is slightly shallower than the salinity minimum

Identification of the LSW as a potential-vorticity minimum permitted TALLEY and MCCARTNEY (1982) to extend the region of identifiable LSW beyond that of the salinity minimum, without encompassing the entire MNADW. North of 41°N, a layer of minimum potential vorticity, centered at 36.88 σ_2, is nearly coincident with the salinity minimum and oxygen maximum South of 41°N, the potential-vorticity minimum remains coincident with a slight oxygen maximum (separated from and above the MNADW) until both the potential-vorticity minimum and secondary oxygen maximum disappear at 38°N

The termination of the salinity minimum at 41°N is remarkably abrupt, resulting in a strong subsurface salinity front with almost vertical isohalines over a depth range exceeding 1000 m. It is coincident with a similar, but less striking, thermal front centered at about 4°C, but the density (σ_2) field exhibits no strong horizontal gradient.

South of the 41°N front, the LSW shifts abruptly to higher density, higher salinity, and lower oxygen and underlies the northernmost strong MOW. The region of the lingering potential-vorticity minimum between 38°N and the 41°N front is also a transitional regime for LSW salinity (Fig. 16). On the vertical sections of potential temperature, salinity and oxygen, this transitional regime appears as a layer, centered at $\sigma_2 \sim 36.9$, of weaker vertical gradients than to the south. The sharply defined northern and southern boundaries may be related to the bottom topography at 41°N (Azores–Biscay Rise) and 37°N (East

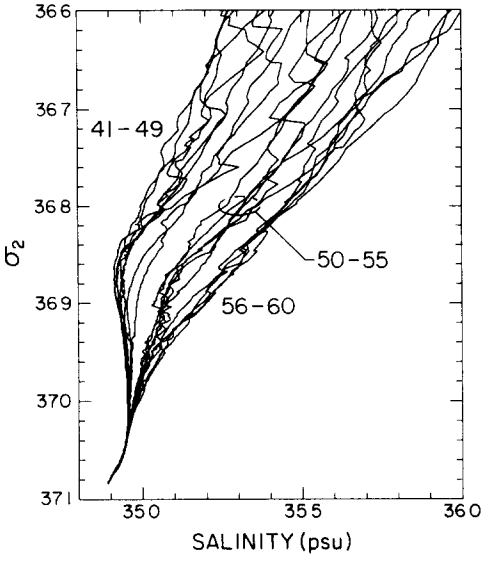

Fig 16 σ_2 vs salinity for OC202 Stas 41–60 (44°59′–35°35′N) Stas 50–55 (40°31′–38°0′N) form the distinct central group at densities 36 8–36 92 σ_2 Fresher Stas 41–49 are characteristic of the LSW and the saltier Stas 56–60 are characteristic of the MOW regime

Azores Fracture Zone). The absence of a salinity minimum is probably due to the high salinity of the overlying MOW. A measure of mixing efficiency is the density ratio (Fig. 15), which has a lateral minimum on the $\sigma_2 = 36.7$ and 36.8 isopycnals in this region. The lowest values are 1.3–1.4, which are well within the salt-fingering regime (SCHMITT, 1981). The lowest density ratio in the region occurs at $\sigma_2 = 36.8$ at Sta. 53, which is the northernmost location of well-developed MOW, and of staircases beneath the MOW (Section 7). The low density ratio suggests that this transitional region is a site of active mixing between the LSW and MOW, which also may account for the downward shift of the oxygen maximum and the disappearance of the nutrient minima

9 ICELAND–SCOTLAND OVERFLOW WATER IN THE ICELAND BASIN

Cold (<3°C), saline (>34.96), dense ($\sigma_\theta > 27.85$, $\sigma_2 > 37.00$), high-oxygen (>6 4 ml l^{-1}) and nutrient-poor water associated with a sharp southward dip of the near-bottom isopycnals and isopleths of all other characteristics from 1500 to 2800 m on the slope south of Iceland is a combination of the cold, dense overflows through the Faroe Bank Channel and across the Iceland–Faroe Rise (WORTHINGTON, 1970, WORTHINGTON, 1976; WARREN, 1981) with entrained thermocline, intermediate and deep waters. We follow SWIFT (1984) in designating this bottom water in the Iceland Basin Iceland–Scotland Overflow Water (ISOW) ISOW also is found in the northern Rockall Trough, but in much smaller volume and with less effect on Atlantic properties. A sharp transition occurs near 60°30′N, between the ISOW to the north and slightly fresher, less-oxygenated variety to the south (Figs 3, 8 and 17). On the northern slope, both salinity and oxygen increase rather noisily from the LSW downward to the highest values (salinities ~34.98; oxygen ~6.5 ml l^{-1}) at the bottom. The vertical gradients of nutrients are weak, but the concentrations generally

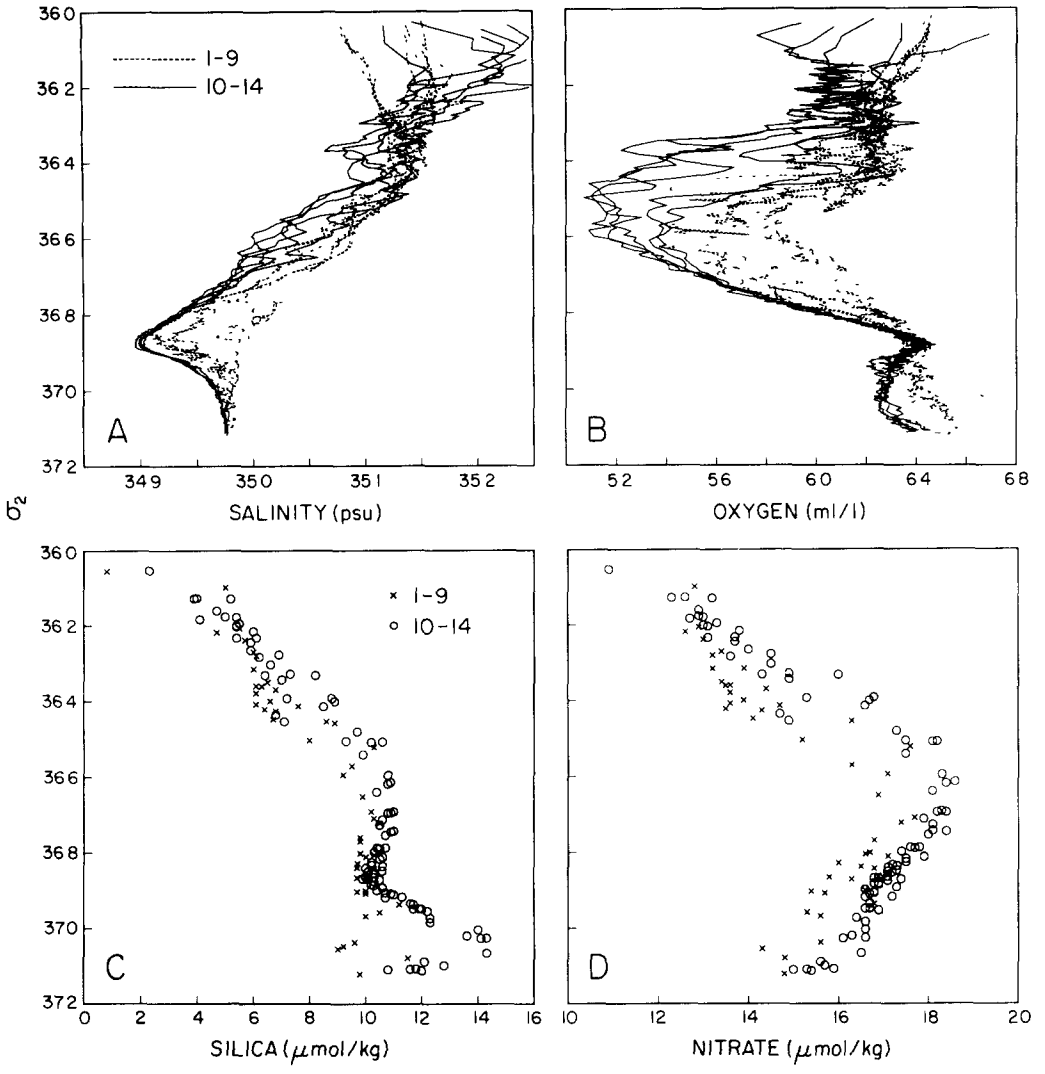

Fig 17 (A) σ_2 vs CTD salinity, (B) σ_2 vs CTD oxygen (ml l^{-1}), (C) σ_2 vs silica (μmol kg^{-1}), and (D) σ_2 vs nitrate (μmol kg^{-1}) for Stas 1–9 (×) and 10–14 (○), spanning the Iceland Basin

decrease toward the bottom. In the southern, deeper half of the Iceland Basin, salinity increases more smoothly downward, and a layer of nearly uniform salinity is found near the bottom, which is slightly fresher than the bottom layer to the north. The oxygen profiles are also smoother than to the north, but show a layer of low oxygen (<6.3 ml l^{-1}) about 500 m thick separating the bottom water from the LSW. Phosphate and nitrate (Figs 10, 11 and 17D) slowly decrease downward to the bottom, but silica shows a maximum (>14 μmol kg^{-1}) about 200 m above the bottom (Figs 9 and 17C). The silica maximum coincides roughly with the layer of low oxygen; the high-silica and low-oxygen concentrations suggest a southern source, as discussed below. The bottom oxygen (~6.4 ml l^{-1}) in the southern Iceland Basin is slightly lower, and the bottom silica (~12 μmol kg^{-1}),

phosphate (~1.0 μmol kg^{-1}), and nitrate (~1.6 μmol kg^{-1}) are somewhat higher than their bottom values to the north.

Because the bottommost water in the Iceland Basin, with a density >37.1 σ_2 (~45.885 σ_4), is denser than any other waters found north of 20°N, one of its sources can only be ISOW from the northern Iceland Basin itself. Of course this is not the pure endmember ISOW coming through the Faroe Bank Channel, which can have a density of >37 4 σ_2 (SWIFT, 1984) and whose silica is <10 μmol kg^{-1} The elevated silica content of the bottom water in the southern Basin (Stas 10–14), relative to the purer ISOW found in the northern half, indicates a larger component of southern water. The oxygen minimum and silica maximum just above the bottom in the southern Iceland Basin must also have a significant component of water from the south since the ISOW, SPMW and LSW are all high in oxygen and low in silica We suggest that this southern water comes from around the southern side of the Rockall Plateau in the deep westward northern boundary current below the eastward-flowing LSW, and has its ultimate origin in the northward eastern boundary current discussed by SAUNDERS (1987) and MCCARTNEY (1991) and below in Section 12. HARVEY and THEODOROU (1986) hypothesized a flow of ISOW from the Rockall Trough into the Iceland Basin; however, the amount of pure ISOW which they estimate following this route seems indistinguishable from zero, being only 12% of 2 5 Sv On the other hand, the cyclonic deep circulation in the Iceland Basin shown by HARVEY and THEODOROU (1986) would account for dense ISOW in the southern part of the Iceland Basin, as recirculating water from the northern Iceland Basin which has undergone additional modification by mixing with overlying waters with a southern source

10. NORTHEAST ATLANTIC DEEP WATERS

Following the nomenclature of LEE and ELLETT (1967), we refer to the deep water underlying the LSW just south of the Rockall Plateau as Northeast Atlantic Deep Water (NEADW). Between the southern slope of the Rockall Plateau and 41°N (Azores–Biscay Rise) in our section, it is marked by a vertical salinity maximum at $\theta \sim 2.9$°C, $\sigma_\theta \sim 27.86$, $\sigma_2 \sim 37.0$ and depth ~2700 m The maximum salinity is highly uniform at slightly above 34.95. South of 41°N, the salinity maximum disappears, and salinity at this density increases slightly (Fig. 18B) due to the influence of overlying MOW. Although no vertical extremum of oxygen or nutrients is associated with the salinity maximum, these characteristics are also nearly uniform along the maximum ($O_2 \sim 6$ 1 ml l^{-1}, SiO_3~20 μmol kg^{-1}, $PO_4 \sim 1.1$ μmol kg^{-1}, and $NO_3 \sim 18$ μmol kg^{-1}).

The salinity maximum itself was taken to be the indentifier of NEADW by ELLETT and MARTIN (1973), who ruled out the MOW as a potential source because of the relatively high oxygen of the NEADW. HARVEY and ARHAN (1988) suggested that ISOW is important in the NEADW makeup in the northern part of this region, but also correctly point to the importance of the deep MOW influence in increasing the salinity and decreasing the oxygen of the NEADW toward the south.

On an isopycnal ($\sigma_2 = 37.0$) that characterizes the salinity maximum, it is clear that salinity is actually lowest in the region where there is a vertical salinity maximum and where the water is commonly referred to as NEADW (Fig. 18B). The NEADW appeared as a positive salinity anomaly in LEE and ELLETT (1965) because it has slightly higher salinity than the western North Atlantic waters used by WORTHINGTON and METCALF (1961) to construct their average potential temperature–salinity curve The deep western North

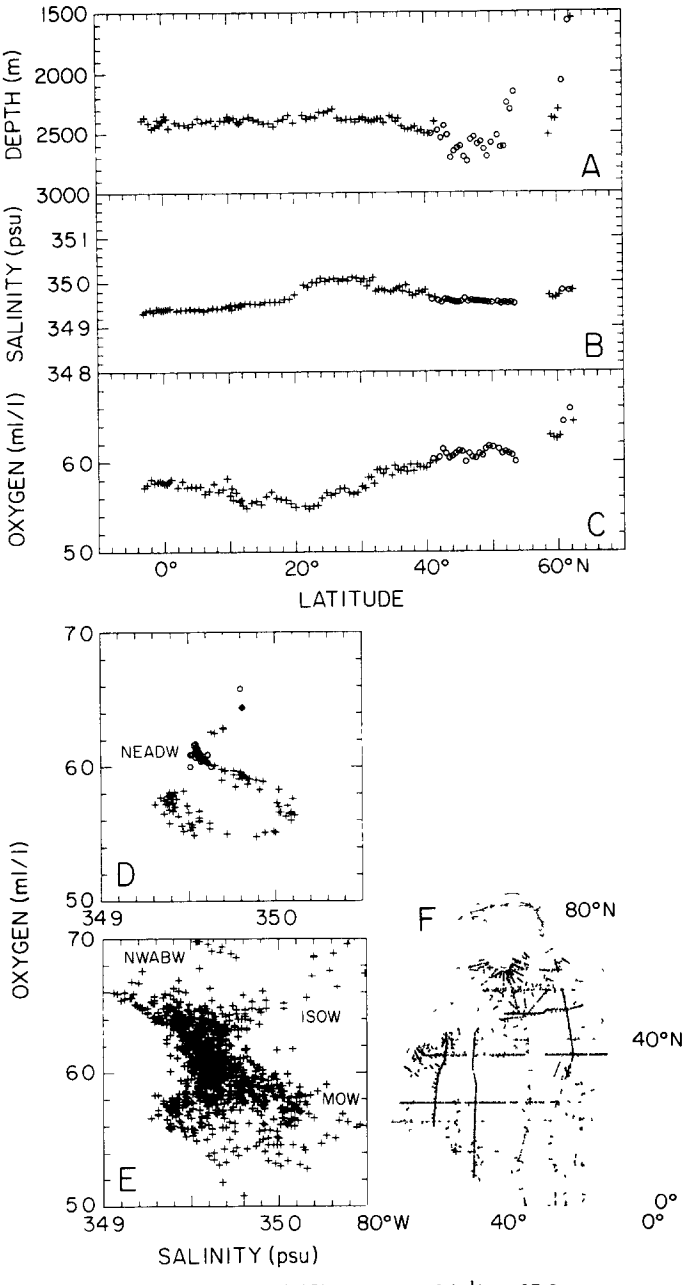

Fig 18 (A) Depth (m), (B) salinity, and (C) oxygen (ml l^{-1}) at 37 0 σ_2, approximately the density of the vertical salinity maximum indicating Northeast Atlantic Deep Water which is found between the Rockall Plateau and 41°N, along the *Oceanus* 202 section Stations where there is a salinity maximum near this density are indicated with circles (D) Oxygen (ml l^{-1}) vs salinity at 37 0 σ_2 for the *Oceanus* 202 stations Water-mass names follow Harvey and Arhan (1988) ISOW indicates the salty, high-oxygen branch, and MOW indicates the salty, low-oxygen branch NEADW is the lower-salinity, intermediate-oxygen point Missing from our section is the NWABW (Lee and Ellett, 1967), but it can be seen in (E) showing oxygen (ml l^{-1}) vs salinity for a selected set of stations from the entire North Atlantic [see (F)]

Atlantic is influenced by Northwest Atlantic Bottom Water (NWABW), which is largely derived from the Denmark Strait overflow and hence is relatively fresh (LEE and ELLETT, 1967). The NEADW's vertical salinity maximum north of 41°N is due to the existence of overlying LSW; south of 41°N, the overlying water is salty MOW and the NEADW's characteristic salinity maximum disappears.

While emphasis has been placed in the past on explaining the NEADW's vertical salinity maximum and positive salinity anomaly relative to the western North Atlantic, it is also necessary to account for its low salinity relative to both the ISOW and MOW influences at this density, as illustrated in Fig. 18D by an oxygen vs salinity diagram based on our section data. Since our section was located too far east to observe NWABW, we include a similar diagram (Fig. 18E) for a selection of stations from the entire North Atlantic, which shows the low-salinity, high-oxygen NWABW as well as ISOW, NEADW and MOW. If, for simplicity, we assume that mixing is largely along this isopycnal and that oxygen is conservative, the NEADW appears to be more a mixture of MOW and NWABW, which has a significant component of the Denmark Strait Overflow Water, with very little ISOW input. We also note that we saw no ISOW influence south of the Rockall Plateau (Section 9), although we are aware that on occasion ISOW has been spotted there, identified by salinity higher than 34.96 at a potential temperature of 3.0°C (WORTHINGTON and WRIGHT, 1970).

Vertical mixing may also be important, to some extent, in raising the salinity of the waters at, say 37 0 σ_2, under the MOW. Salinity at the vertical maximum between the overlying LSW and the underlying Antarctic Bottom Water (Section 12) may be decreased by vertical mixing

11 NORTH ATLANTIC DEEP WATER

WUST (1935) designated the intermediate salinity maximum derived from and including the MOW as the Upper North Atlantic Deep Water (UNADW) Well-developed MOW appears in our section between 22 and 40°N, as discussed in Section 7. South of 22°N, the salinity maximum is truncated from above by the AAIW's salinity minimum The salinity maximum here is much colder (~5°C), less saline (~35.1), and somewhat denser ($\sigma_\theta \sim 27.7$; $\sigma_1 \sim 32\ 3$; $\sigma_2 \sim 36.8$) than the high-salinity core of the MOW

The UNADW extends at a depth of 1500–1800 m (generally shallower in the north and deeper in the south) all the way to the south end of the section. The maximum salinity decreases southward to 34 96 ($\theta \sim 3.6$°C) near 6°N and increases again farther south. However, σ_θ remains at 27.7–27.8 ($\sigma_2 \sim 36.8$–36 9) There is an isolated core of high salinity (>34.98) centered slightly south of the equator A similar core of high chlorofluorocarbons (CFC) is observed at the same location (BULLISTER, 1989; DONEY and BULLISTER, 1992). These cores indicate that the UNADW reaches the equator in the southward western boundary undercurrent of the North Atlantic and turns to the east to flow along the equator (WEISS *et al* , 1985)

The UNADW south of 22°N also is characterized by a minimum of dissolved silica; a tongue of low silica similar in appearance to that of high salinity is found under the high-silica tongue associated with the AAIW The silica concentration along the axis of the low-silica tongue does not increase monotonically southward but instead shows lateral minima at some latitudes. The most conspicuous of these is centered at the equator, with a silica

concentration <18 μmol kg^{-1} within 2° of the equator. This core evidently indicates the eastward flow of the UNADW that has reached the equator along the western boundary as already deduced from the salinity and CFC distributions. There are three isolated cores (<20 μmol kg^{-1}) at 7–14°N, but the isolation may be due to the coarse vertical spacing of samples (400 m) at the intervening stations, which may have missed the absolute minimum. Nevertheless, the lateral maximum found at 6°N (Sta. 106) is coincident with lower salinities (~34.96), described previously, and could be taken as evidence of a westward flow Between 15 and 18°N, the minimum concentration is definitely higher than that to the north and south, and a lateral maximum (>23 μmol kg^{-1}) occurs at 15°30'N (Sta. 93). This maximum may indicate westward flow of higher-silica water, whose ultimate origin is not obvious. The maximum salinity, however, shows a monotonic southward decrease at these latitudes.

Below the salinity maximum and silica minimum is an oxygen maximum, which is part of the oxygen maximum found throughout the section and is identified as MNADW. North of 41°N, where its oxygen content is highest, it is identical with LSW. Oxygen at the maximum drops beneath the MOW and reaches a lateral minimum at about 20°N, where its depth is about 3000 m ($\sigma_\theta \sim 27.88$; $\sigma_2 \sim 37.04$). South of 20°N, the oxygen content rises again and the depth of the maximum decreases to about 2000 m ($\sigma_\theta \sim 27.84$; $\sigma_2 \sim 36.98$)

Just north and south of the equator are found two cores of high oxygen (>5.8 ml l^{-1}). The splitting of the equatorial core may be associated with a peak in the Mid-Atlantic Ridge. (At this longitude the Mid-Atlantic Ridge runs east–west along the equator.) There is also a narrow band of laterally higher oxygen (>5.8 ml l^{-1}) at 10°N (Sta. 101) although the vertical maximum is only weakly developed here. This high-oxygen water extends down to the bottom, where it joins a larger amount of high-oxygen water (>5.8 ml l^{-1}) in the south.

That the vertical oxygen maximum in low latitudes is not a direct southward continuation along 25°W of the high-latitude maximum associated with the LSW is obvious from the lateral minimum of oxygen (<5.6 ml l^{-1}) near 20°N, which is tilted downward to the south and extends down to the bottom. Similarly, an interruption of the oxygen maximum of the MNADW is found between 18 and 30°N on the GEOSECS western Atlantic section (Bainbridge, 1980). A more recent section along 35°W also shows a low-oxygen region (<5.7 ml l^{-1}) from 2000 m to the bottom centered at 22°N (McCartney *et al.*, 1991). This separation of the high-oxygen water by an intervening lower-oxygen region in mid-latitudes can be seen clearly on the maps of oxygen at the core of the MNADW (Wust, 1935) and along isopycnals nearly coinciding with it (Reid, 1981; Kawase and Sarmiento, 1986). These maps indicate that the high-oxygen LSW flows southward along the western boundary, as well as eastward across the North Atlantic (Section 8; also Talley and McCartney, 1982). Upon reaching the equator, part of the southward-flowing high-oxygen water leaves the coast and continues to the east along the equator. Thus, the mid-latitude region is comparatively less well-aerated

The oxygen maximum of the MNADW is associated with similar minima of phosphate and nitrate.

Another deeper oxygen maximum is very well defined at ~3700 m against the southern flank of the Mid-Atlantic Ridge, south of the equator. Here a core of high oxygen (>6 ml l^{-1}) is found at $\sigma_4 \sim 45\ 87$. The maximum weakens and continues to the north of the Ridge as far as 10°N. This deep oxygen maximum represents the Lower North Atlantic Deep Water (LNADW) described by Wust (1935). Farther north, the deep oxygen maximum is

not recognized clearly except for a weak indication at 18–20°N. A large body of water with nearly uniform oxygen (5.6–5.7 ml l^{-1}) is found below the MNADW between 20°N and the Azores–Biscay Rise (42°N). Other properties are also fairly uniform here, suggesting that a single source controlled by the bottom topography and vertical mixing determine the properties of this water.

The deep oxygen maximum south of the Mid-Atlantic Ridge coincides with clearly defined minima of all three nutrients ($SiO_3 < 34$ μmol kg^{-1}, $PO_4 < 1.4$ μmol kg^{-1}, and $NO_3 < 21$ μmol kg^{-1}) Because there is no water with these characteristics at this density level in the South Atlantic (REID, 1989, Fig. 36), the isolated high-oxygen, low-nutrient water constrained to the southern flank of the Ridge must be supplied by the western boundary current from the North Atlantic. The source of this water appears to be the Denmark Strait Overflow Water (EDMOND and ANDERSON, 1971; REID and LYNN, 1971).

North of the Mid-Atlantic Ridge, the nutrients do not show clear minima corresponding to the deep oxygen maximum

The oxygen minimum (<5 8 ml l^{-1}) that separates the maxima of the MNADW and LNADW is located at $\sigma_3 \sim 41.47$ ($\sigma_2 \sim 37.04$; depth ~2800 m) and is very clearly defined south of the Mid-Atlantic Ridge In this region it coincides with a weak minimum of salinity and well-defined maxima of the nutrients, as was observed earlier by EDMOND and ANDERSON (1971). Farther north, the oxygen minimum is only weakly developed but extends as far as 10°N at a somewhat greater depth. WUST (1935) remarked only briefly on this minimum, but REID *et al* (1977) and REID (1989) described it in some detail The origin and route of this lower-oxygen, higher-nutrient water are not immediately obvious, but its ultimate source appears to be the Circumpolar Water (REID, 1989, REID and MANTYLA, 1989).

12 ANTARCTIC BOTTOM WATER

Except for the core of the LNADW pressed against the southern flank of the Mid-Atlantic Ridge south of the equator (Section 11), the ISOW that is found at the bottom of the Iceland Basin (Section 9), and the shallow bottom water over the Rockall Plateau, all the near-bottom water in this section is of South Atlantic origin Even ISOW in the southern Iceland Basin has a significant component from the south, as is apparent in its elevated silica content relative to the actual overflow water, and the northern North Atlantic water masses, LSW and SPMW, with which it mixes. Although this dense (cold) water from the south is commonly referred to as the Antarctic Bottom Water (AABW) (WUST, 1935), it does not derive directly from the densest Antarctic water formed in the Weddell Sea but from the less dense Lower Circumpolar Water (MANTYLA and REID, 1983; REID, 1989). The Lower Circumpolar Water is colder, fresher, poorer in oxygen, and richer in nutrients than the North Atlantic Deep Water (NADW), and its northward spreading as the AABW can be traced by these characteristics

South of the Mid-Atlantic Ridge, which is located at the equator, and below the oxygen maximum and nutrient minima of the LNADW, temperature, salinity and oxygen decrease, and nutrients increase very sharply downward These strong vertical gradients in the characteristics begin at $\theta \sim 2$°C (BROECKER *et al.*, 1976) and are generally taken to be the boundary between the NADW and the AABW (WRIGHT, 1970). The bottom characteristics south of the equator at $\theta \sim 0$ 22°C, $S \sim 34$ 70, $\sigma_4 \sim 46$ 04, $O_2 \sim 5$ 10 ml l^{-1}, $SiO_3 \sim 114$ μmol kg^{-1}, $PO_4 \sim 2.4$ μmol kg^{-1}, and $NO_3 \sim 32$ μmol kg^{-1}. This water is the

coldest (newest) form of the AABW seen in this section. Whether it is flowing east along the southern flank of the Mid-Atlantic Ridge toward the Romanche Gap or flowing west to cross the equator into the Guiana Basin* farther west is not clear.

The second coldest bottom water in this section is found near 11°N in the Cape Verde Basin, east of the Vema Fracture Zone. Here the bottom characteristics are $\theta \sim 1.77$°C, $S \sim 34.87$, $\sigma_4 \sim 45.90$, $O_2 \sim 5.72$ ml l^{-1}, $SiO_3 \sim 51$ μmol kg^{-1}, $PO_4 \sim 1.5$ μmol kg^{-1}, and $NO_3 \sim 22$ μmol kg^{-1}. There is a slight oxygen maximum at the bottom, overlain by a minimum at ~4500 m. This water comes from the Guiana Basin through the Vema Fracture Zone across the Mid-Atlantic Ridge, and flows almost due east in the Cape Verde Basin (McCartney *et al.*, 1991). Part of the water that emerges from the Fracture Zone turns to the north along the eastern flank of the Mid-Atlantic Ridge and provides the main source of water that flows into the basins farther north in the eastern North Atlantic (Mantyla and Reid, 1983; McCartney *et al.*, 1991). By the time it reaches the deep Canary Basin near 23°N in our section, its characteristics are altered to $\theta \sim 1.95$°C, $S \sim 34.88$, $\sigma_4 \sim 45.87$, $O_2 \sim 5.63$ ml l^{-1}, $SiO_3 \sim 47$ μmol kg^{-1}, $PO_4 \sim 1.45$ μmol kg^{-1}, and $NO_3 \sim 22$ μmol kg^{-1}, due principally to vertical mixing with the overlying NADW.

Farther north in the Iberian and West European Basins, where the bottom water is overlain by the high-salinity, high-oxygen NEADW (Section 10), the bottom characteristics are $\theta \sim 2.15$°C, $S \sim 34.91$, $\sigma_4 \sim 45.86$, $O_2 \sim 5.55$ ml l^{-1}, $SiO_3 \sim 44$ μmol kg^{-1}, $PO_4 \sim 1.4$ μmol kg^{-1}, and $NO_3 \sim 21$ μmol kg^{-1}. North of the Azores–Biscay Rise (42°N), oxygen below 4000 m is decreased to <5.6 ml l^{-1}. On Mantyla and Reid's (1983) bottom-oxygen map this low-oxygen water is shown as isolated in the West European Basin. However, McCartney *et al.* (1991) show water with oxygen <5.6 ml l^{-1} at the eastern boundary from the Cape Verde Basin at least as far north as 36°N. Thus it appears that low-oxygen north of the Azores–Biscay Rise comes from the south along the eastern boundary.

This eastern boundary current carrying the purest (coldest) AABW is found in the Canary Basin north of 32°N, flows northward through the Discovery Gap at the eastern end of the East Azores Fracture Zone (Saunders, 1987), and on northward to at least 53°N (McCartney, submitted). The bottom water becomes warmer and decreases in oxygen and silica along the way. Based on vertical geostrophic shear and deep-water properties, it appears that this flow extends up to at least the 2.5°C isotherm near the Rockall Trough. In the Rockall Trough, the flow turns westward and is found in our section between the Rockall Plateau, where the isopycnals slope steeply, and Sta. 38, where the isopycnals are deepest; there is no obvious change in properties at Sta. 38, so presumably the westward-flowing water recirculates in this relatively enclosed region. A level of no motion above the bottom water is indicated; direct current measurements by Dickson *et al.* (1985) showed a level of no zonal flow at 2000–2500 m at the south slope of the Rockall Plateau.

Part of the deep flow south of the Rockall Plateau turns northward into the Iceland Basin, providing water of low oxygen and high silica which mixes with the ISOW. This narrow northward flow of high-silica AABW is clearly shown in a section extending from Greenland to Rockall Plateau by Mann *et al.* (1973). This is the source of the oxygen minimum and silica maximum found near 2600 m in the southern Iceland Basin in our section

*The names of the basins in this section follow those used by Mantyla and Reid (1983)

13 SUMMARY

Various features of the property distributions observed along a quasi-meridional transect of closely-spaced stations spanning the entire circulation regime in the eastern Atlantic Ocean have been described and interpreted in terms of the large-scale circulation. The more important results are listed below.

(1) In the Subpolar Mode Water, the northward increase in density following the local minimum in potential vorticity supports the McCARTNEY and TALLEY (1982) scenario for the formation of SPMW. However, only one station of very well-mixed SPMW was found in this closely-spaced section South of 47°N, the predominant SPMW is the well-known 11–12°C water, which is found to 27°N. There is a suggestion of recirculation of this lightest SPMW in the tropics, where a pycnostad of appropriate density is found between 6 and 15°N

(2) A thermostad (pycnostad) with a temperature 8–9°C is observed at ~400 m within 2° of the equator. This thermostad lies beneath the secondary thermocline marking the bottom of the Equatorial 13°C Water thermostad. Although it has not been noted before, examination of previous data suggests that it is a ubiquitous feature along the equator of the Atlantic Ocean.

(3) The distribution of properties on the isopycnals intersecting the Antarctic Intermediate Water and low-salinity water above the Mediterranean Outflow Water supports the conjecture of the northern influence of the AAIW

(4) The MOW salinity maximum is seen to have a great deal of lateral structure, with a number of lobes of high salinity. Two Meddies were observed, well south of the main MOW and at lower density

(5) The close station spacing clearly reveals abrupt water-mass boundaries, e.g. the southern edge of the Labrador Sea Water, which changes abruptly at the Azores–Biscay Rise Closer examination of the LSW using potential vorticity indicates a region south of the main LSW where mixing between MOW and LSW may be especially active, the southern boundary of this region is associated with the East Azores Fracture Zone.

(6) The close station spacing also reveals a sharp demarcation in the central Iceland Basin between the newest Iceland–Scotland Overflow Water and older bottom water. The older water is characterized by reduced oxygen and elevated silica, indicating a larger component of southern water.

(7) The Northeast Atlantic Deep Water is recognized as a salinity maximum at ~2700 m beneath the LSW and extends from the Rockall Plateau to the Azores–Biscay Rise The NEADW appears to be a mixture of the MOW and the Northwest Atlantic Bottom Water, which has a significant component of the Denmark Strait Overflow Water, with very little input from ISOW.

(8) An isolated core of high-salinity, low-silica Upper North Atlantic Deep Water is observed at the equator indicating that the UNADW, that has reached the equator along the western boundary undercurrent, turns to the east to flow along the equator. This finding is consistent with the observations of chlorofluorocarbons by WEISS *et al.* (1985) and DONEY and BULLISTER (1992).

(9) A core of the high-oxygen, low-nutrient Lower North Atlantic Deep Water is found pressed against the southern flank of the Mid-Atlantic Ridge south of the equator This water appears to originate in the Denmark Strait Overflow Water and must have come by way of the southward western boundary undercurrent and an eastward flow along the equator

(10) The oxygen minimum that separates the maxima of the Middle North Atlantic Deep Water and LNADW is clearly defined south of the Mid-Atlantic Ridge. It is associated with a weak minimum of salinity and well-defined maxima of nutrients confirming the earlier observations by EDMOND and ANDERSON (1971) and supports the hypothesis that it originates from high southern latitudes.

(11) There is a large body of nearly homogeneous water below the MNADW between 20°N and the Azores–Biscay Rise. A single source determined by the bottom topography and vertical mixing may be the cause of the near homogeneity of this water.

(12) The observed bottom-water characteristics are consistent with the previous finding that the near-bottom water in the eastern basin is of South Atlantic origin (MANTYLA and REID, 1983; MCCARTNEY *et al* , 1991). A westward northern boundary current is clearly indicated by all properties on the southern slope of the Rockall Plateau and appears to be the downstream continuation of the northward eastern boundary current found from the Canary Basin northward to the Rockall Trough (SAUNDERS, 1987; MCCARTNEY, submitted)

Acknowledgements—This study was supported by the National Science Foundation under Grant OCE86-14486 The skillful technical support provided by the Oceanographic Data Facility at Scripps Institution of Oceanography and the nutrient chemistry group of Oregon State University was essential to the success of the field program We thank Captain Howland and the crew of R V *Oceanus* for their cooperation and dedication, and J L Reid, A W Mantyla and R G Peterson for reviewing the manuscript Martha Denham assisted with computations This is Contribution No 7723 from the Woods Hole Oceanographic Institution

REFERENCES

ARHAN M (1990) The North Atlantic Current and Subarctic Intermediate Water *Journal of Marine Research*, **48**, 109–144

ARMI L and H STOMMEL (1983) Four views of a portion of the North Atlantic subtropical gyre *Journal of Physical Oceanography*, **13**, 828–857

ARMI L and W ZENK (1984) Large lenses of highly saline Mediterranean Water *Journal of Physical Oceanography*, **14**, 1560–1576

BAINBRIDGE A E (1980) *GEOSECS Atlantic Expedition, Vol 2, Sections and profiles* National Science Foundation, Washington, DC 198 pp

BROECKER W S , T TAKAHASHI and Y -H LI (1976) Hydrography of the central Atlantic—I The two-degree discontinuity *Deep-Sea Research*, **23**, 1083–1104

BUBNOV V A , V D EGORIKHIN, Z N MATVEEVA, S E NAVROTSKAYA and D I FILIPPOV (1979) Graphical presentation of the USSR oceanographic observations in the tropical Atlantic during GATE (June to September, 1974) RSMAS, University of Miami, Technical Report, TR 79-1, 163 pp

BULLISTER J L (1989) Chlorofluorocarbons as time-dependent tracers in the ocean *Oceanography*, **2(2)**, 12–17

COCHRANE J D (1975) Portions of a proposal for research on the North Equatorial Countercurrent system of the Atlantic Ocean Texas A&M University, Technical Report, 75-7-T, 112 pp

COCHRANE J D , F J KELLY JR and C R OLLING (1979) Subthermocline countercurrents in the western equatorial Atlantic Ocean *Journal of Physical Oceanography*, **9**, 724–738

CRAIG H and T HAYWARD (1987) Oxygen supersaturation in the ocean biological versus physical contribution *Science*, **235**, 199–202

DICKSON R R , W J GOULD, T J MULLER and C MAILLARD (1985) Estimates of the mean circulation in the deep (>2000 m) layer of the eastern North Atlantic *Progress in Oceanography*, **14**, 103–128

DONEY S C and J L BULLISTER (1992) A chlorofluorocarbon section in the eastern North Atlantic *Deep-Sea Research*, **39**, 1857–1883

DUING W , P HISARD, E KATZ, J MEINCKE, L MILLER, K V MOROSHKIN, G PHILANDER, A A RIBNIKOV, K VOIGT and R WEISBERG (1975) Meanders and long waves in the equatorial Atlantic *Nature*, **257**, 280–284

DUING W , F OSTAPOFF and J MERLE, editors (1980) *Physical oceanography of the tropical Atlantic during GATE* University of Miami, 117 pp

EDMOND J M and G C ANDERSON (1971) On the structure of the North Atlantic Deep Water *Deep-Sea Research*, **18**, 127–133

ELLETT D J and J H A MARTIN (1973) The physical and chemical oceanography of the Rockall Channel *Deep-Sea Research*, **20**, 585–625

FAHRBACH E , J MEINCKE and A SY (1986) Observations of the horizontal separation of the salinity core and the current core in the Atlantic Equatorial Undercurrent *Journal of Marine Research*, **44**, 763–779

HARVEY J and M ARHAN (1988) The water masses of the central North Atlantic in 1983–84 *Journal of Physical Oceanography*, **18**, 1855–1875

HARVEY J G and A THEODOROU (1986) The circulation of Norwegian Sea overflow in the eastern North Atlantic *Oceanologica Acta*, **2**, 393–402

HENIN C , P HISARD and B PITON (1986) Observations hydrologiques dans l'Océan Atlantique équatorial (juillet 1982–août 1984) FOCAL, Vol 1, *Travaux et Documents, ORSTROM*, **196**, 1–191

HISARD P , J CITEAU and A MORLIÈRE (1976) Les système des contre-courants équatoriaux subsuperficiels permanence et extension de la branche sud dans l'ocean Atlantique *Cahiers ORSTROM, Série Océanographie*, **14**, 209–220

IVERS W D (1975) The deep circulation in the northern North Atlantic, with especial reference to the Labrador Sea PhD dissertation, University of California, San Diego, 179 pp

JENKINS W J and J C GOLDMAN (1985) Seasonal oxygen cycling and primary production in the Sargasso Sea *Journal of Marine Research*, **43**, 465–491

KAWASE M and J L SARMIENTO (1986) Circulation and nutrients in middepth Atlantic waters *Journal of Geophysical Research*, **91**, 9749–9770

KELLY F J JR (1978) Currents and waters at 140 cl t^{-1} in the western equatorial Atlantic during February–March–April M S thesis, Texas A&M University, 59 pp

KHANAICHENKO N K (1980) *The system of the equatorial countercurrents in the ocean* Oxonian Press, New Delhi, 158 pp

KOLESNIKOV A G , editor (1973) *Oceanographic atlas, equalant* I & II, Physical Oceanography, UNESCO, Paris, Vol 1, 289 pp

LEE A and D ELLETT (1965) On the contribution of overflow water from the Norwegian Sea to the hydrographic structure of the North Atlantic Ocean *Deep-Sea Research*, **12**, 129–142

LEE A and D ELLETT (1967) On the water masses of the Northwest Atlantic Ocean *Deep-Sea Research*, **14**, 183–190

LUYTEN J R , J PEDLOSKY and H STOMMEL (1983) The ventilated thermocline *Journal of Physical Oceanography*, **13**, 292–309

MANN C R , A R COOTE and D M GARNER (1973) The meridional distribution of silicate in the western Atlantic Ocean *Deep-Sea Research*, **20**, 791–801

MANTYLA A W and J L REID (1983) Abyssal characteristics of the World Ocean Waters *Deep-Sea Research*, **30**, 805–833

MCCARTNEY M S (1982) The subtropical recirculation of Mode Waters *Journal of Marine Research*, **40**(suppl), 427–464

MCCARTNEY M S (Submitted) Recirculating components to the deep boundary current of the northern North Atlantic *Progress in Oceanography*

MCCARTNEY M S and L D TALLEY (1982) The Subpolar Mode Water of the North Atlantic Ocean *Journal of Physical Oceanography*, **12**, 1169–1188

MCCARTNEY M S , S L BENNETT and M E WOODGATE-JONES (1991) Eastward flow through the Mid-Atlantic Ridge at 11°N and its influence on the abyss of the eastern basin *Journal of Physical Oceanography*, **21**, 1089–1121

MCDOWELL S E and H T ROSSBY (1978) Mediterranean water an intense mesoscale eddy off the Bahamas *Science*, **202**, 1085–1087

MERLE J (1978) Atlas hydrologique saisonnier de l'Océan Atlantique intertropical *Travaux et Documents, ORSTOM*, **82**, 1–184

METCALF W G (1969) Dissolved silicate in the deep North Atlantic *Deep-Sea Research*, **16**(suppl), 139–145

METCALF W G and M C STALCUP (1967) Origin of the Atlantic Equatorial Undercurrent *Journal of Geophysical Research*, **72**, 4959–4975

METCALF W G , A D VOORHIS and M C STALCUP (1962) The Atlantic Equatorial Undercurrent *Journal of Geophysical Research*, **67**, 2499–2508

MONTGOMERY R B (1938) Circulation in upper layers of southern North Atlantic deduced with use of isentropic analysis *Papers in Physical Oceanography and Meteorology*, **6(2)**, 1–55

REID J L JR (1962) Distribution of dissolved oxygen in the summer thermocline *Journal of Marine Research*, **20**, 138–148

REID J L (1979) On the contribution of the Mediterranean Sea outflow to the Norwegian–Greenland Sea *Deep-Sea Research*, **26**, 1199–1223

REID J L (1981) On the mid-depth circulation of the world ocean In *Evolution of physical oceanography, scientific surveys in honor of Henry Stommel*, MIT Press, Cambridge, MA, pp 70–111

REID J L (1989) On the total geostrophic circulation of the South Atlantic Ocean Flow patterns, tracers, and transport *Progress in Oceanography*, **23**, 149–244

REID J L and R J LYNN (1971) On the influence of the Norwegian–Greenland and Weddell seas upon the bottom waters of the Indian and Pacific oceans *Deep-Sea Research*, **18**, 1063–1088

REID J L and A W MANTYLA (1989) Circumpolar water in the North Atlantic (abstr) *Eos*, **70**, 1132

REID J L , W D NOWLIN JR and W C PATZERT (1977) On the characteristics and circulation of the southwestern Atlantic Ocean *Journal of Physical Oceanography*, **7**, 62–91

RICHARDSON P L , M S MCCARTNEY and C MAILLARD (1991) A search for Meddies in historical data *Dynamics of Atmospheres and Oceans*, **15**,241–265

ROEMMICH D and C WUNSCH (1985) Two transatlantic sections meridional circulation and heat flux in the subtropical North Atlantic Ocean *Deep-Sea Research*, **32**, 619–664

SAUNDERS P M (1987) Flow through Discovery Gap *Journal of Physical Oceanography*, **17**, 631–643

SCHMITT R W (1981) Form of temperature–salinity relationship in the Central Water evidence for double-diffusive mixing *Journal of Physical Oceanography*, **11**, 1015–1026

SHULENBERGER E and J L REID (1981) The Pacific shallow oxygen maximum, deep chlorophyll maximum, and primary productivity, reconsidered *Deep-Sea Research*, **28**, 901–919

SIEDLER G , A KUHL and W ZENK (1987) The Madeira Mode Water *Journal of Physical Oceanography*, **17**, 1561–1570

SWIFT J H (1984) The circulation of the Denmark Strait and Iceland–Scotland overflow waters in the North Atlantic *Deep-Sea Research*, **31**, 1339–1355

TALLEY L D and M S MCCARTNEY (1982) Distribution and circulation of Labrador Sea Water *Journal of Physical Oceanography*, **12**, 1189–1205

TSUCHIYA M (1986) Thermostads and circulation in the upper layer of the Atlantic Ocean *Progress in Oceanography*, **16**, 235–267

TSUCHIYA M (1989) Circulation of the Antarctic Intermediate Water in the North Atlantic Ocean *Journal of Marine Research*, **47**, 747–755

WARREN B A (1981) Deep circulation of the world ocean In *Evolution of physical oceanography, scientific surveys in honor of Henry Stommel*, MIT Press, Cambridge, MA, pp 6–41

WEISS R F , J L BULLISTER, R H GAMMON and M J WARNER (1985) Atmospheric chlorofluoromethanes in the deep equatorial Atlantic *Nature*, **314**, 608–610

WORTHINGTON L V (1970) The Norwegian Sea as a mediterranean basin *Deep-Sea Research*, **17**, 77–84

WORTHINGTON L V (1976) On the North Atlantic circulation *Johns Hopkins Oceanographic Studies*, **6**, 1–110

WORTHINGTON L V and W G METCALF (1961) The relationship between potential temperature and salinity in deep Atlantic water *Rapports et Procès-verbaux des Réunion Conseil Permanent International pour l'Exploration de la Mer*, **149**, 122–128

WORTHINGTON L V and W R WRIGHT (1970) North Atlantic Ocean atlas of potential temperature, salinity in the deep water including temperature, salinity and oxygen profiles from Erika Dan cruises of 1962 *The Woods Hole Oceanographic Institution Atlas Series*, **2**, 1–24 + 58 plates

WRIGHT W R (1970) Northward transport of Antarctic Bottom Water in the western Atlantic Ocean *Deep-Sea Research*, **17**, 367–371

WUST G (1935) Schichtung und Zirkulation des Atlantischen Ozeans Die Stratosphare des Atlantischen Ozeans Wissenschaftliche Ergebnisse der Deutschen Atlantischen Expedition auf dem Forschungs- und Vermessungsschiff *Meteor* 1925–1927, Vol 6(2), pp 109–288